Synthesis, Characterization, and Molecular Structures of Diethylnitrosamine Metalloporphyrin Complexes of Iron, Ruthenium, and Osmium

Li Chen, Geun-Bae Yi, Li-Sheng Wang, Udeni R. Dharmawardana, Amelia C. Dart, Masood A. Khan, and George B. Richter-Addo*

Department of Chemistry and Biochemistry, University of Oklahoma, 620 Parrington Oval, Norman, Oklahoma 73019

Received February 10, 1998

Diethylnitrosamine reacts with $[(TPP)Fe(THF)_2]ClO_4$ (TPP = 5,10,15,20-tetraphenylporphyrinato dianion) in toluene to generate the bis-nitrosamine complex, $[(TPP)Fe(Et_2NNO)_2]ClO_4$, in 96% isolated yield. The related $[(TTP)Fe(Et_2NNO)_2]SbF_6$ (TTP = 5,10,15,20-tetra-*p*-tolylporphyrinato dianion) complex is prepared in 70% isolated yield via a similar reaction in CH_2Cl_2. Reaction of $[(TPP)Fe(Et_2NNO)_2]ClO_4$ in CH_2Cl_2 with NO gas results in the displacement of one of the Et_2NNO ligands to give the air-sensitive and thermally sensitive $[(TPP)Fe(NO)(Et_2NNO)]ClO_4$ derivative. Reaction of (OEP)Ru(CO) (OEP = 2,3,7,8,12,13,17,18-octaethylporphyrinato dianion) with $NOBF_4$ in CH_2Cl_2 gives $[(OEP)Ru(NO)(H_2O)]BF_4$ as the final isolated product (after exposure to air) in 71% isolated yield. The aqua ligand is then displaced by Et_2NNO in CH_2Cl_2 to give $[(OEP)Ru(NO)(Et_2NNO)]BF_4$ in 82% isolated yield. The valence isoelectronic $(OEP)Ru(CO)(Et_2NNO)$ compound is prepared in 71% isolated yield by the addition of excess Et_2NNO to (OEP)Ru(CO) in CH_2Cl_2. The nitrosyl amine complex $[(OEP)Ru(NO)(HNEt_2)]BF_4$ is prepared (i) in 78% yield by diethylamine addition to $[(OEP)Ru(NO)(H_2O)]BF_4$ or (ii) in 71% isolated yield by diethylamine addition to $[(OEP)Ru(NO)(Et_2NNO)]BF_4$. The osmium nitrosamine complexes, $(TTP)Os(CO)(Et_2NNO)$ and $(OEP)Os(CO)(Et_2NNO)$, are prepared in 74% and 66% yields, respectively, by diethylnitrosamine addition to the precursor (porphyrin)Os(CO) compounds in CH_2Cl_2. The nitrosyl $[(OEP)Os(NO)(Et_2NNO)]BF_4$ derivative is prepared in quantitative yield (by IR and ^1H NMR spectroscopy) by the reaction of $(OEP)Os(CO)(Et_2NNO)$ with $NOBF_4$. Labeling studies using $^{15}NOBF_4$, $Et_2N^{15}NO$, and $Et_2NN^{18}O$ have been used to assign the nitrosyl and nitrosamine bands in the IR spectra of several of the complexes. The solid-state structures of $[(TPP)Fe(THF)_2]ClO_4$, $[(TPP)Fe(Et_2NNO)_2]ClO_4$, $[(OEP)Ru(NO)(H_2O)]BF_4$, $(OEP)Ru(CO)(Et_2NNO)$, and $(TTP)Os(CO)(Et_2NNO)$ have also been determined by single-crystal X-ray diffraction. The Et_2NNO ligands display a rare η^1-O binding mode in all three nitrosamine complexes.

Nitrosamines ($R_2NN{=}O$) belong to the family of *N*-nitroso compounds, and they are generally considered to be carcinogenic.[1−7] They are metabolized by cytochrome P450, and final metabolized products may result from initial hydroxylation or denitrosation of the nitrosamine.[8−10] Two types of interactions of nitrosamines with cytochrome P450 have been proposed. The first is the interaction of the nitrosamine with the substrate pocket (type I) prior to the enzyme-catalyzed oxidation,[8,9] and the second is the direct interaction of the nitrosamine with the iron center of the heme (type II) in the enzyme.[8,11] This variable binding of nitrosamines to the heme pocket of cytochrome P450 contributes to the rather complex metabolic pathways of nitrosamine activation.

We were intrigued by the possibility of the direct interaction of nitrosamines with the iron center of cytochrome P450. Although nitrosamines are known to form complexes with some metals,[12−19] no report of the nature of nitrosamine binding to heme or heme models had been documented prior to our study. Interestingly, it has been documented that *N*-hydroxyethylprotoporphyrin IX forms in the livers of mice after diethylnitrosamine treatment, although the mechanism of such formation remains unclear.[20] Some iron nitrosyl porphyrins also nitrosate

(1) Preussman, R.; Stewart, B. W. In *Chemical Carcinogens*, 2nd ed.; C. E. Searle, Ed.; American Chemical Society: Washington, DC, 1984; Vol. 2; pp 643−828.
(2) *Nitrosamines: Toxicology and Microbiology*; Hill, M. J., Ed.; VCH Ellis Horwood Ltd.: Chichester, England, 1988.
(3) Lijinsky, W. *Chemistry and Biology of N-Nitroso Compounds*; Cambridge University Press: Cambridge, 1992.
(4) Cadogan, J. I. G. *Acc. Chem. Res.* **1971**, *4*, 186−192.
(5) Fridman, A. L.; Mukhametshin, F. M.; Novikov, S. S. *Russ. Chem. Rev. (Engl. Transl.)* **1971**, *40*, 34−50.
(6) *Safety Evaluation of Nitrosatable Drugs and Chemicals*; Gibson, G. G.; Ioannides, C., Ed.; Taylor and Francis Ltd.: London, 1981.
(7) Saavedra, J. E. *Org. Prep. Proced. Int.* **1987**, *19*, 83−159.
(8) Ioannides, C.; Gibson, G. G. In *Safety Evaluation of Nitrosatable Drugs and Chemicals*; Gibson, G. G., Ioannides, C., Ed.; Taylor and Francis: London, 1981; pp 257−278.
(9) Guttenplan, J. B. *Mutat. Res.* **1987**, *186*, 81−134.
(10) *Nitrosamines and Related N-Nitroso Compounds. Chemistry and Biochemistry*; Loeppky, R. N., Michejda, C. J., Ed.; American Chemical Society: Washington, DC, 1994; Vol. 553.
(11) Appel, K. E.; Ruf, H. H.; Mahr, B.; Schwarz, M.; Rickart, R.; Kunz, W. *Chem.-Biol. Interact.* **1979**, *28*, 17−33.
(12) Schmidpeter, A.; Nöth, H. *Inorg. Chim. Acta* **1998**, *269*, 7−12.
(13) Asaji, T.; Sakai, H.; Nakamura, D. *Inorg. Chem.* **1983**, *22*, 202−206.
(14) Schmidpeter, A. *Chem. Ber.* **1963**, *96*, 3275−3279.
(15) (a) Klement, U. *Acta Crystallogr.* **1969**, *B25*, 2460−2465. (b) Klement, U.; Schmidpeter, A. *Angew. Chem., Int. Ed. Engl.* **1968**, *7*, 470.
(16) Brown, R. D.; Coates, G. E. *J. Chem. Soc.* **1962**, 4723−4724.
(17) Willett, R. D. *Acta Crystallogr.* **1988**, *B44*, 503−508.
(18) Asaji, T.; Ikeda, R.; Inoue, M.; Nakamura, D. *J. Mol. Struct.* **1980**, *58*, 315−322.
(19) Khan, M. I.; Agarwala, U. C. *Bull. Chem. Soc. Jpn.* **1986**, *59*, 1285−1286.
(20) White, I. N. H.; Smith, A. G.; Farmer, P. B. *Biochem. J.* **1983**, *212*, 599−608.

S0020-1669(98)00159-1 CCC: $15.00
Published on Web 08/20/1998

secondary amines to form nitrosamines.[21,22] Thus, we were interested in (i) preparing discrete adducts of nitrosamines with heme models and (ii) determining the nature of nitrosamine binding to the metal center in such heme models.

The O atom of nitrosamines (R_2NNO) is known to interact with protons,[23−27] carbocations,[28−33] and other electrophiles.[14,31,34,35] The nitroso N atom may also bind to metals in metallacycle complexes.[36,37] The amino N atom may also be protonated.[25] Recently, nitrosamines were shown to form crystalline donor−acceptor complexes with electron acceptors such as DDQ.[38]

We recently communicated our preliminary finding that diethylnitrosamine binds to Fe^{III} and Ru^{II} porphyrins via a unique O-binding mode.[39,40] We now report the full details of our findings and also show that such nitrosamine binding can be successfully extended to include osmium porphyrins. We also report our single-crystal X-ray crystallographic studies on the nitrosamine metalloporphyrin complexes of all three group 8 metals. To the best of our knowledge, these represent the first isolable metalloporphyrin complexes containing nitrosamines as ligands.

Experimental Section

General Procedures. All reactions were performed under an atmosphere of prepurified nitrogen (Airgas) using standard Schlenk techniques and/or in an Innovative Technology Labmaster 100 drybox unless stated otherwise. Solvents were distilled from appropriate drying agents under nitrogen just prior to use: CH_2Cl_2 (CaH_2), THF (Na/benzophenone), toluene (Na), hexane (Na/benzophenone/tetraglyme).

Chemicals. *N*-Nitrosodiethylamine (>99%) was purchased from Fluka. $NOBF_4$, diethylamine (98%), and sodium nitrite (97%) were purchased from Aldrich Chemical Co. and used as received. [^{18}O]Water (97% isotopic purity) was purchased from Isotec. $^{15}NOBF_4$ was synthesized by following published procedures[41] using $Na^{15}NO_2$ (Matheson, 99.4%). (TTP)Os(CO),[42] (OEP)Os(CO),[42] (TPP)FeCl, and (TTP)FeCl[43] (TPP = 5,10,15,20-tetraphenylporphyrinato dianion, TTP = 5,10,15,20-tetra-*p*-tolylporphyrinato dianion, OEP = 2,3,7,8,12,13,-17,18-octaethylporphyrinato dianion) were prepared by following the reported procedures. (OEP)Ru(CO) was obtained from Aldrich Chemical Co. Chloroform-*d* (99.8%), methylene-d_2 chloride (99.9%), and benzene-d_6 (99.6%) were obtained from Cambridge Isotope Laboratories, subjected to three freeze−pump−thaw cycles, and stored over Linde 4 Å molecular sieves. Elemental analyses were performed by Atlantic Microlab, Norcross, GA. Nitric oxide (98%, Matheson Gas) was passed through KOH pellets and a cold trap (dry ice/acetone) to remove higher nitrogen oxides.

Instrumentation. Infrared spectra were recorded on a BioRad FT-155 FTIR spectrometer. ^{1}H NMR spectra were obtained on a Varian XL-300 spectrometer, and the signals were referenced to the residual signal of the solvent employed. All coupling constants are in hertz. FAB mass spectra were obtained on a VG-ZAB-E mass spectrometer. Solution magnetic susceptibilities were measured using the Evans NMR method.[44]

Synthesis of [^{18}O]Et_2NNO. This procedure is a slight modification of a published procedure for the preparation of the analogous $Me_2NN^{18}O$.[25] Sodium nitrite (0.154 g) was dissolved in [^{18}O]water (1 g), and the mixture was deaerated by repeated freeze−pump−thaw cycles. The sample was placed under nitrogen and immersed in an ice bath. Anhydrous HCl gas was passed through the mixture for several minutes until the weight increase was approximately 0.2 g and a yellow precipitate was observed to form. The sample was stirred for an additional 7 h. Cold Et_2NH (0.35 g, ice bath) was added, and the mixture was stirred overnight under nitrogen. The resulting mixture was extracted with CH_2Cl_2 (15 mL), and the extract was dried over anhydrous $MgSO_4$ (to remove any remaining [^{18}O]water). The solution was filtered into another container, and the solvent was removed by passage of N_2 gas through the filtrate. Low-resolution mass spectrum (EI): *m*/*z* 104 $[Et_2NN^{18}O]^+$ (100), 102 $[Et_2NNO]^+$ (14).

Preparation of [(TPP)Fe(THF)$_2$]ClO$_4$. To a stirred THF solution (40 mL) of (TPP)FeCl (0.400 g, 0.568 mmol) was added $AgClO_4 \cdot H_2O$ (0.118 g, 0.568 mmol). The solution turned from brown to red. The solution was heated to a gentle boil for 5 min. The solution was filtered, and hexane (10 mL) was added to the filtrate. The resulting solution was placed in a freezer (−22 °C) overnight. The violet crystalline solid that formed was collected by filtration, washed with hexane (3 × 10 mL), and dried in vacuo for 10 min (0.423 g, 0.483 mmol, 85%). Anal. Calcd for $C_{52}H_{44}N_4O_6ClFe \cdot 0.5H_2O$: C, 67.79; H, 4.92; N, 6.03. Found: C, 67.76; H, 4.54; N, 6.30. IR (KBr, cm^{-1}): ν_{ClO_4} 1094 br s and 622 m; also 1597 m, 1484 m, 1442 m, 1337 m, 1225 w, 1200 m, 1177 m, 1005 s, 906 w br, 857 m, 805 s, 755 s, 730 w, 718 w, 704 s, 661 s, 525 m. μ_{eff} (C_6D_6) = 5.4.

Preparation of [(TPP)Fe(THF)$_2$]SbF$_6$·THF. To a stirred THF solution (30 mL) of (TPP)FeCl (0.200 g, 0.284 mmol) was added $AgSbF_6$ (0.098 g, 0.285 mmol). The solution turned from brown to red. The solution was heated to a gentle boil for 30 min. The solution was filtered, and then hexane (60 mL) was added to the filtrate. The resulting solution was placed in a freezer (−22 °C) overnight. The violet crystalline solid that formed was collected by filtration, washed with hexane (2 × 15 mL), and dried in vacuo for 10 min (0.248 g, 0.221 mmol, 88% yield). Anal. Calcd for $C_{44}H_{28}N_4FeSbF_6 \cdot 3C_4H_8O$: C, 60.02; H, 4.68; N, 5.00. Found: C, 60.02; H, 5.08; N, 4.80. IR (KBr, cm^{-1}): ν_{SbF_6} 656 vs; also 1598 m, 1577 w, 1484 m, 1444 m, 1339 m, 1201 m, 1177 m, 1065 m, 1006 s, 997 m, 921 w br, 904 w br, 862 m, 804 s, 757 s, 729 m, 717 m, 707 s, 522 w. μ_{eff} (CD_2Cl_2) = 5.8.

Preparation of [(TPP)Fe(Et$_2$NNO)$_2$]ClO$_4$. To a toluene solution (40 mL) of [(TPP)Fe(THF)$_2$]ClO_4 (0.200 g, 0.219 mmol) was added Et_2NNO (0.5 mL, ca. 5 mmol), and the reaction mixture was stirred for 10 min. The color changed from brown-purple to red-purple, and fine red-purple microcrystals precipitated. Hexane (40 mL) was slowly

(21) Bonnett, R.; Charalambides, A. A.; Martin, R. A. *J. Chem. Soc., Perkin Trans. 1* **1978**, 974−980.
(22) Bonnett, R.; Charalambides, A. A.; Martin, R. A.; Sales, K. D.; Fitzsimmons, B. W. *J. Chem. Soc., Chem. Commun.* **1975**, 884−885.
(23) Keefer, L. K.; Ohannesian, L.; Hrabie, J. A. *J. Org. Chem.* **1989**, *54*, 2432−2436.
(24) Keefer, L. K.; Hrabie, J. A.; Ohannesian, L.; Flippen-Anderson, J. L.; George, C. *J. Am. Chem. Soc.* **1988**, *110*, 3701−3702.
(25) Keefer, L. K.; Hrabie, J. A.; Hilton, B. D.; Wilbur, D. *J. Am. Chem. Soc.* **1988**, *110*, 7459−7462.
(26) Nguyen, M. T.; Hegarty, A. F. *J. Chem. Soc., Perkin Trans. 2* **1987**, 345−349.
(27) Axenrod, T. *Spectrosc. Lett.* **1970**, *3*, 263−265.
(28) Schmidpeter, A. *Tetrahedron Lett.* **1963**, 1421−1424.
(29) Stöldt, E.; Kreher, R. *Chem. Ber.* **1983**, *116*, 819−822.
(30) Hünig, S.; Geldern, L.; Lücke, E. *Angew. Chem., Int. Ed. Engl.* **1963**, *2*, 327−328.
(31) Klamann, D.; Koser, W. *Angew. Chem., Int. Ed. Engl.* **1963**, *2*, 741−742.
(32) Hünig, S.; Büttner, G.; Cramer, J.; Geldern, L.; Hansen, H.; Lücke, E. *Chem. Ber.* **1969**, *102*, 2093−2108.
(33) Büttner, G.; Hünig, S. *Chem. Ber.* **1971**, *104*, 1088−1103.
(34) Perry, R. A.; Chow, Y. L. *Can. J. Chem.* **1974**, *52*, 315−324.
(35) Fraser, R. R.; Wigfield, Y. Y. *Tetrahedron Lett.* **1971**, 2515−2518.
(36) Albinati, A.; Affolter, S.; Pregosin, P. S. *J. Organomet. Chem.* **1990**, *395*, 231−254.
(37) Constable, A. G.; McDonald, W. S.; Shaw, B. L. *J. Chem. Soc., Dalton Trans.* **1980**, 2282−2287.
(38) Greer, M. L.; Blackstock, S. C. *J. Am. Chem. Soc.* **1997**, *119*, 11343−11344.
(39) Yi, G.-B.; Khan, M. A.; Richter-Addo, G. B. *J. Am. Chem. Soc.* **1995**, *117*, 7850−7851.
(40) Yi, G.-B.; Khan, M. A.; Richter-Addo, G. B. *Inorg. Chem.* **1996**, *35*, 3453−3454.
(41) Connelly, N. G.; Draggett, P. T.; Green, M.; Kuc, T. A. *J. Chem. Soc., Dalton Trans.* **1977**, 70−73.
(42) Che, C.-M.; Poon, C.-K.; Chung, W.-C.; Gray, H. B. *Inorg. Chem.* **1985**, *24*, 1277−1278.
(43) Adler, A. D.; Longo, F. R.; Kampas, F.; Kim, J. *J. Inorg. Nucl. Chem.* **1970**, *32*, 2443−2445.
(44) Grant, D. H. *J. Chem. Educ.* **1995**, *72*, 39−40 and references therein.

added to complete the precipitation of the red-purple microcrystals. The supernatant solution was discarded, and the solid was dried in vacuo to give $[(TPP)Fe(Et_2NNO)_2]ClO_4$ (0.204 g, 0.210 mmol, 96% yield) as dark-purple microcrystals. Crystals for X-ray diffraction studies were grown at −20 °C from a CH_2Cl_2/hexane (3:1) mixture. Anal. Calcd for $C_{52}H_{48}N_8O_6ClFe$: C, 64.23; H, 4.98; N, 11.52. Found: C, 64.28; H, 5.11; N, 11.36. IR (KBr, cm^{-1}): $\nu_{NO/NN}$ = 1270 m; also 3056 w, 2984 w, 2941 w, 1597 m, 1480 m, 1441 m, 1421 w, 1380 w, 1335 m, 1201 m, 1178 w, 1097 br s, 1074 s, 1007 vs, 997 m, 953 w, 803 s, 755 s, 736 m, 719 m, 704 s, 661 m, 624 m. Low-resolution mass spectrum (FAB): *m*/*z* 668 $[(TPP)Fe]^+$ (100). μ_{eff} (C_6D_6) = 5.9.

$[(TPP)Fe(Et_2N^{15}NO)_2]ClO_4$. IR (KBr, cm^{-1}): $\nu^{15}_{NO/N^{15}N}$ = 1254 m.

Preparation of $[(TPP)Fe(Me_2NNS)_2]ClO_4$. This air-sensitive complex was prepared similarly from the reaction of Me_2NNS[45] with $[(TPP)Fe(THF)_2]ClO_4$. Anal. Calcd for $C_{48}H_{40}N_8O_4ClS_2Fe$: C, 60.79; H, 4.25; N, 11.82; S, 6.76. Found: C, 60.92; H, 4.64; N, 10.94; S, 7.04. IR (KBr, cm^{-1}): ν1596 m, 1488 m, 1440 m, 1393 m, 1373 m, 1342 w, 1202 m, 1160 m, 1120 s, 1099 br vs, 1075 sh, 997 s, 874 w, 797 s, 766 s, 754 s, 736 m, 711 m, 704 s, 664 m, 623 s, 528 m. Low-resolution mass spectrum (FAB): *m*/*z* 668 $[(TPP)Fe]^+$ (100). Low-resolution mass spectrum (70 eV DIP): *m*/*z* 90 $[Me_2NNS]^+$ (100), 75 $[MeNNS]^+$ (40).

Preparation of $[(TTP)Fe(Et_2NNO)_2]SbF_6$. To a stirred CH_2Cl_2 solution (10 mL) of $[(TTP)Fe(THF)_2]SbF_6$ (0.100 g, 0.090 mmol) was added Et_2NNO (0.5 mL, ca. 5 mmol). The solution was stirred for 30 min, and hexane (20 mL) was added. The product mixture was stored at −22 °C overnight. Precipitation of the solid was enhanced by mixing of the CH_2Cl_2/hexane solution, and the supernatant solution was discarded. The solid product remaining was washed with hexane (3 × 10 mL) and dried in vacuo for 10 min to give analytically pure $[(TTP)Fe(Et_2NNO)_2]SbF_6$ as dark purple crystals (0.073 g, 0.063 mmol, 70% yield). Anal. Calcd for $C_{56}H_{56}O_2N_8FeSbF_6$: C, 57.75; H, 4.85; N, 9.62. Found: C, 57.73; H, 4.87; N, 9.57. IR (KBr, cm^{-1}): ν_{NO} 1271 m, ν_{NN} 1256 m; ν_{SbF_6} 657 s; also 3025 w, 2986 w, 2943 w, 2921 w, 1476 m, 1451 w, 1379 w, 1331 w, 1200 m, 1182 m, 1128 w, 1108 w, 1098 w, 1073 w, 1004 s, 953 w, 849 w, 843 w, 805 s, 724 m, 680 w, 595 w, 567 w, 527 w, 517 w, 426 w. Low-resolution mass spectrum (FAB): *m*/*z* 724 $[(TTP)Fe]^+$ (100). Low-resolution mass spectrum (70 eV EI): *m*/*z* 102 $[Et_2NNO]^+$ (100%). μ_{eff} (C_6D_6) = 6.0.

$[(TTP)Fe(Et_2N^{15}NO)_2]SbF_6$. IR (KBr, cm^{-1}): ν^{15}_{NO} 1262 m, $\nu_{N^{15}N}$ 1249 m.

Attempted Preparation of $[(TPP)Fe(NO)(Et_2NNO)]ClO_4$. Nitric oxide was bubbled through a CH_2Cl_2 solution (30 mL) of $[(TPP)Fe(Et_2NNO)_2]ClO_4$ (0.100 g, 0.10 mmol) for 5 min. During this time, the color of the mixture changed from red-purple to light-red. After the volume of solution was reduced to ca. 10 mL, hexane (3 mL) was slowly added. Cooling the reaction mixture at −22 °C overnight resulted in the formation of a precipitate formulated as $[(TPP)Fe(NO)(Et_2NNO)]ClO_4$, which was isolated by filtration as dark-purple microcrystals (0.064 g, 0.07 mmol, 72%). IR (KBr, cm^{-1}): ν_{NO} 1916 s, $\nu_{NO/NN}$ (Et_2NNO) 1268 m; also 3056 w, 3027 w, 2987 w, 1599 m, 1575 w, 1484 m, 1442 m, 1381 w, 1348 m, 1310 w, 1202 m, 1180 w, 1697 br s, 1009 s, 801 s, 755 s, 734 s, 704 s, 666 m, 623 m. ^1H NMR ($CDCl_3$): δ 8.94 (br s, pyrrole H of TPP), 8.26 (br, *m*/*p*-H of TPP), 7.83 (br, *o*-H of TPP), 4.22 (br, CH_3CH_2NNO), 2.56 (br, CH_3CH_2NNO), 0.72 (br, CH_3CH_2NNO), −0.18 (br, CH_3CH_2NNO). This product readily lost the axial NO ligand at ambient temperature to give a solid formulated as $[(TPP)Fe(Et_2NNO)]ClO_4 \cdot 0.5CH_2Cl_2$. Anal. Calcd for $C_{49}H_{39}N_7O_6Cl_2Fe$: C, 61.79; H, 4.17; N, 10.40. Found: C, 62.13; H, 4.48; N, 10.36.

Preparation of $[(OEP)Ru(NO)(H_2O)]BF_4$. To a stirred CH_2Cl_2 (30 mL) solution of (OEP)Ru(CO) (0.200 g, 0.302 mmol) was added $NOBF_4$ (0.036 g, 0.31 mmol). The solution was stirred for 20 min, during which time the mixture turned from reddish pink to brown red. The crude product was obtained by removal of the solvent in vacuo. Crystallization of this crude product by evaporation of a CH_2Cl_2/hexane (20 mL, 1:1) solution in air yielded $[(OEP)Ru(NO)(H_2O)]BF_4 \cdot H_2O \cdot 0.4CH_2Cl_2$ (0.178 g, 0.217 mmol, 71%). Anal. Calcd for $C_{36}H_{46}O_2N_5F_4BRu \cdot H_2O \cdot 0.4CH_2Cl_2$: C, 53.28; H, 5.99; N, 8.53. Found: C, 53.28; H, 6.11; N, 8.14. IR (KBr, cm^{-1}): ν_{NO} 1852 s; also 2965 s, 2934 m, 2872 m, 1471 m, 1455 m, 1380 w, 1376 w, 1316 w, 1272 m, 1228 w, 1154 s, 1110 s br, 1084 s br, 1058 s, 1022 s, 995 s, 964 s, 925 vw, 843 m, 795 w, 747 m, 731 m, 714 m, 696 w. ^1H NMR ($CDCl_3$): δ 10.53 (s, 4H, *meso*-H of OEP), 5.32 (s, 0.8H, CH_2Cl_2), 4.22 (q, *J* = 7, 16H, CH_2CH_3 of OEP), 2.02 (t, *J* = 7, 24H, CH_2CH_3 of OEP). The peak for H_2O was not observed, or may be masked by other peaks. Low-resolution mass spectrum (FAB): *m*/*z* 664 $[(OEP)Ru(NO)]^+$ (100), 634 $[(OEP)Ru]^+$ (46).

Preparation of $[(OEP)Ru(NO)(Et_2NNO)]BF_4$. A stirred CH_2Cl_2 solution (10 mL) of $[(OEP)Ru(NO)(H_2O)]BF_4 \cdot H_2O \cdot 0.4CH_2Cl_2$ (0.070 g, 0.085 mmol) was reacted with Et_2NNO (0.50 mL, 4.6 mmol) for 5 min, during which time the red-brown mixture darkened. Hexane (5 mL) was then added, and the mixture was kept at −20 °C for 3 days to result in the precipitation of $[(OEP)Ru(NO)(Et_2NNO)]BF_4$. The crystals of $[(OEP)Ru(NO)(Et_2NNO)]BF_4$ were isolated by decanting the supernatant solution and drying the solid in vacuo (0.060 g, 0.070 mmol, 82%). Anal. Calcd for $C_{40}H_{54}O_2N_7BF_4Ru$: C, 56.34; H, 6.38; N, 11.50. Found: C, 56.30; H, 6.33; N, 11.43. IR (KBr, cm^{-1}): ν_{NO} 1847 s, ν_{NO} (Et_2NNO) 1250 m, ν_{NN} (Et_2NNO) 1201 m; also 2965 s, 2934 m, 2873 m, 1495 m, 1469 m, 1454 m, 1432 m, 1375 m, 1318 w, 1271 m, 1250 s, 1201 m, 1154 s, 1111 w, 1058 s br, 1021 s, 995 s, 964 m, 846 m, 747 m, 731 m, 714 m, 682 m, 617 w. ^1H NMR ($CDCl_3$): δ 10.47 (s, 4H, *meso*-H of OEP), 4.21 (q, *J* = 7, 16H, CH_2CH_3 of OEP), 1.97 (t, *J* = 7, 24H, CH_2CH_3 of OEP), 1.94 (q, *J* = 7, 2H, CH_3CH_2NNO (overlap with OEP)), 0.58 (q, *J* = 7, 2H, CH_3CH_2NNO), −0.50 (t, *J* = 7, 3H, CH_3CH_2NNO), −1.98 (t, *J* = 7, 3H, CH_3CH_2NNO). Low-resolution mass spectrum (FAB): *m*/*z* 664 $[(OEP)Ru(NO)]^+$ (100), 634 $[(OEP)Ru]^+$ (33).

$[(OEP)Ru(NO)(Et_2N^{15}NO)]BF_4$. IR (KBr, cm^{-1}): ν^{15}_{NO} 1234 m, $\nu_{N^{15}N}$ 1194 m.

$[(OEP)Ru(NO)(Et_2NN^{18}O)]BF_4$. IR (KBr, cm^{-1}): $\nu_{N^{18}O}$ 1240 m.

Preparation of $[(OEP)Ru(^{15}NO)(Et_2NNO)]BF_4$. To a stirred CH_2Cl_2 (10 mL) solution of $(OEP)Ru(CO)(Et_2NNO)$ (0.013 g, 0.017 mmol) was added $^{15}NOBF_4$ (0.002 g, 0.017 mmol). The solution was gently heated for 10 min, and all of the solvent was removed. A ^1H NMR spectrum of the product indicated the quantitative nature of the reaction to produce $[(OEP)Ru(^{15}NO)(Et_2NNO)]BF_4$. IR (KBr, cm^{-1}): ν^{15}_{NO} 1808 s. Low-resolution mass spectrum (FAB): *m*/*z* 665 $[(OEP)Ru(^{15}NO)]^+$ (100), 634 $[(OEP)Ru]^+$ (34).

Preparation of $(OEP)Ru(CO)(Et_2NNO)$. A stirred CH_2Cl_2 (5 mL) solution of (OEP)Ru(CO) (0.070 g, 0.106 mmol) was reacted with Et_2NNO (0.30 mL, 2.8 mmol) for 10 min, during which time the mixture turned from red to pink red. Hexane (10 mL) was added. Two kinds of crystals (red needles and dark red cubes) were obtained by cooling the mixture at −20 °C for 5 days. The ^1H NMR spectrum of the mixed crystals (0.065 g) showed the presence of $(OEP)Ru(CO)(Et_2NNO)$ and unreacted (OEP)Ru(CO) in a 9:1 ratio. The needles (the desired $(OEP)Ru(CO)(Et_2NNO)$ product) and cubes (unreacted (OEP)Ru(CO)) were then separated by hand-picking, and the red needles so obtained were identified as $(OEP)Ru(CO)(Et_2NNO) \cdot 0.2CH_2Cl_2$ (0.059 g, 0.075 mmol, 71%). This product is also obtained in quantitative yield by heating the reaction mixture to its boiling point (ca. 40 °C) for 10 min. Anal. Calcd for $C_{41}H_{54}O_2N_6Ru \cdot 0.2CH_2Cl_2$: C, 63.37; H, 7.02; N, 10.76. Found: C, 63.11; H, 7.00; N, 10.76. IR (KBr, cm^{-1}): ν_{CO} 1910 s, ν_{NO} 1301 m, ν_{NN} 1257 m; also 2961 s, 2931 s, 2868 m, 1540 w, 1484 w, 1466 m, 1448 m, 1378 m, 1370 m, 1358 w, 1319 m, 1272 m, 1229 m, 1211 w, 1148 s, 1110 m, 1056 s, 1018 s, 991 s, 960 s, 921 w, 858 w, 840 s, 829 m, 746 s, 714 m, 702 w, 669 w. ^1H NMR ($CDCl_3$): δ 9.96 (s, 4H, *meso*-H of OEP), 5.28 (s, 0.4H, CH_2Cl_2), 4.02 (q, *J* = 7, 16H, CH_2CH_3 of OEP), 3.40 (q, *J* = 7, 2H, CH_3CH_2NNO), 2.64 (q, *J* = 7, 2H, CH_3CH_2NNO), 1.89 (t, *J* = 7, 24H, CH_2CH_3 of OEP), 0.91 (t, *J* = 7, 3H, CH_3CH_2NNO), 0.25 (t, *J* = 7, 3H, CH_3CH_2NNO). Low-resolution mass spectrum (FAB): *m*/*z* 662 $[(OEP)Ru(CO)]^+$ (88), 634 $[(OEP)Ru]^+$ (100).

$(OEP)Ru(CO)(Et_2N^{15}NO)$. IR (KBr, cm^{-1}): ν^{15}_{NO} 1287 m, $\nu_{N^{15}N}$ 1248 m.

$(OEP)Ru(CO)(Et_2NN^{18}O)$. IR (KBr, cm^{-1}): $\nu_{N^{18}O}$ 1284 m.

Preparation of $[(OEP)Ru(NO)(HNEt_2)]BF_4$. Method I: To a stirred CH_2Cl_2 (5 mL) solution of $[(OEP)Ru(NO)(H_2O)]BF_4 \cdot H_2O \cdot 0.4CH_2$-

(45) Middleton, W. J. *J. Am. Chem. Soc.* **1966**, *88*, 3842−3844.

Cl_2 (0.100 g, 0.122 mmol) was added $HNEt_2$ (0.50 mL, 4.8 mmol). The solution was stirred for 10 min, during which time the mixture turned from brown red to reddish pink. Hexane (5 mL) was then added, and the mixture was kept at −20 °C for 2 days to result in the precipitation of crystals of $[(OEP)Ru(NO)(HNEt_2)]BF_4$, which were isolated by discarding the supernatant solution and drying the solid in vacuo (0.082 g, 0.095 mmol, 78% yield). Suitable crystals for elemental analysis were obtained as $[(OEP)Ru(NO)(HNEt_2)]BF_4 \cdot 2H_2O$ by crystallization in air.

Method II: To a stirred CH_2Cl_2 (3 mL) solution of $[(OEP)Ru(NO)(Et_2NNO)]BF_4$ (0.015 g, 0.018 mmol) was added $HNEt_2$ (0.20 mL, 1.9 mmol). The solution was stirred for 30 min, during which time the mixture turned from brown red to reddish pink. Hexane (5 mL) was then added, and the solution was allowed to evaporate to dryness in air in the fume hood. Crystals of $[(OEP)Ru(NO)(HNEt_2)]BF_4$ were then obtained (0.011 g, 0.013 mmol, 71% yield). Anal. Calcd for $C_{40}H_{55}ON_6F_4BRu \cdot 2H_2O$: C, 55.88; H, 6.92; N, 9.77. Found: C, 55.47; H, 6.77; N, 9.77. IR (KBr, cm^{-1}): ν_{NO} 1824 s, ν_{NH} 3156 m br; also 2967 s, 2933 m, 2872 m, 1471 m, 1456 m, 1372 m, 1318 m, 1276 m, 1229 w, 1153 s, 1110 s, 1056 s br, 1020 s, 993 s, 964 s, 913 w, 848 m, 815 m, 750 m, 730 w, 712 m, 669 vw, 522 s. ^1H NMR ($CDCl_3$): δ 10.37 (s, 4H, *meso*-H of OEP), 4.17 (m, 16H, CH_2CH_3 of OEP), 1.99 (t, $J = 7$, 24H, CH_2CH_3 of OEP), 0.95 (br, 4H, $HN(CH_2CH_3)_2$), −0.58 (br, 6H, $HN(CH_2CH_3)_2$). The amine proton signal was not observed and may be masked by other peaks. Low-resolution mass spectrum (FAB): *m*/*z* 664 $[(OEP)Ru(NO)]^+$ (100), 634 $[(OEP)Ru]^+$ (48).

Preparation of (TTP)Os(CO)(Et$_2$NNO). To a CH_2Cl_2 (10 mL) solution of (TTP)Os(CO) (0.035 g, 0.039 mmol) was added Et_2NNO (0.2 mL, ca. 2 mmol). The solution was gently heated and stirred for 20 min. All of the solvent was then removed. The product was recrystallized from CH_2Cl_2/hexane (3 mL, 1:2) at −20 °C overnight. The supernatant was discarded, and the black purple crystalline solid was washed with hexane (3 × 10 mL). The solid was dried in vacuo for 2 h to give $(TTP)Os(CO)(Et_2NNO) \cdot 0.5$hexane (0.030 g, 0.029 mmol, 74% yield). Anal. Calcd for $C_{53}H_{46}O_2N_6Os \cdot 0.5C_6H_{14}$: C, 65.16; H, 5.17; N, 8.14. Found: C, 65.13; H, 5.20; N, 8.53. IR (KBr, cm^{-1}): ν_{CO} 1902 s, ν_{NO} 1292 m, ν_{NN} 1251 m; also 3021 w, 2955 w, 2920 w, 2870 w, 1799 w, 1609 w, 1571 w, 1531 m, 1513 w, 1454 w, 1437 w, 1412 w, 1380 w, 1352 m, 1307 w, 1208 w, 1180 m, 1118 w, 1107 w, 1069 m, 1011 s, 953 w, 798 s, 714 m, 675 w, 644 w, 596 w, 561 w, 525 m, 453 w. ^1H NMR ($CDCl_3$): δ 8.50 (s, 8H, pyrrole H of TTP), 8.11 (d, $J = 8$, 4H, *o*-H of TTP), 7.86 (d, $J = 8$, 4H, *o*′-H of TTP), 7.50 (d, $J = 8$, 4H, *m*-H of TTP), 7.44 (d, $J = 8$, 4H, *m*′-H of TTP), 2.65 (s, 12H, CH_3 of TTP), 1.25 (br, hexane), 0.86 (t, hexane). The Et peaks of Et_2NNO were not observed at room temperature. ^1H NMR (CD_2Cl_2, −10 °C): δ 8.57 (s, 8H, pyrrole H of TTP), 8.14 (d, $J = 7$, 4H, *o*-H of TTP), 7.87 (d, $J = 7$, *o*′-H of TTP), 7.57 (d, $J = 7$, *m*-H of TTP), 7.51 (d, $J = 7$, *m*′-H of TTP), 2.68 (s, 12H, CH_3 of TTP), 2.19 (q, $J = 7$, 2H, CH_3CH_2NNO), 1.27 (br, hexane), 1.03 (q, $J = 7$, 2H, CH_3CH_2NNO), 0.88 (t, hexane), 0.06 (t, $J = 7$, 3H, CH_3CH_2NNO), −1.26 (t, $J = 7$, 3H, CH_3CH_2NNO). Low-resolution mass spectrum (FAB): *m*/*z* 887 $[(TTP)Os(CO)]^+$ (32), 859 $[(TTP)Os]^+$ (41). Low-resolution mass spectrum (70 eV EI): *m*/*z* 102 $[Et_2NNO]^+$ (100). A suitable crystal for structure determination was grown by recrystallization of the compound from a CH_2Cl_2/hexane mixture at −20 °C.

(TTP)Os(CO)(Et$_2$N^{15}NO). IR (KBr, cm^{-1}): ν^{15}_{NO} 1275 m, $\nu_{N^{15}N}$ 1246 m.

Preparation of (OEP)Os(CO)(Et$_2$NNO). This product was prepared in 66% yield in a manner analogous to the TTP derivative described above. Anal. Calcd for $C_{41}H_{54}O_2N_6Os$: C, 57.72; H, 6.38; N, 9.85. Found: C, 57.61; H, 6.40; N, 8.59. IR (KBr, cm^{-1}): ν_{CO} 1883 s, ν_{NO} 1294 m, ν_{NN} 1222 m; also 2962 w, 2933 w, 2870 w, 1587 w, 1544 w, 1537 w, 1513 w, 1488 w, 1464 m, 1454 s, 1374 m, 1354 w, 1336 w, 1313 w, 1273 m, 1231 m, 1209 m, 1149 m, 1111 w, 1056 s, 992 m, 959 s, 859 w, 842 m, 826 w, 744 s, 712 m, 707 m, 685 w, 654 w, 600 w, 542 w. ^1H NMR ($CDCl_3$): δ 9.68 (s, 4H, pyrrole H of OEP), 3.93 (m, 16H, CH_2CH_3 of OEP), 1.85 (t, $J = 8$, 24H, CH_2CH_3 of OEP). The Et peaks of Et_2NNO were not observed at room temperature. ^1H NMR (CD_2Cl_2, −40 °C): δ 9.76 (s, 4H, pyrrole H of OEP), 3.98 (m, 16H, CH_2CH_3 of OEP), 1.85 (t, $J = 7.5$, 24H, CH_2CH_3 of OEP), 1.85 (q, 2H, CH_3CH_2NNO, overlapping with OEP), 0.68 (q, $J = 7.5$, 2H, CH_3CH_2NNO), −0.11 (t, $J = 7$, 3H, CH_3CH_2NNO), −1.69 (t, $J = 7$, 3H, CH_3CH_2NNO). Low-resolution mass spectrum (FAB): *m*/*z* 751 $[(OEP)Os(CO)]^+$ (13), 723 $[(OEP)Os]^+$ (6). Low-resolution mass spectrum (70 eV EI): *m*/*z* 102 $[Et_2NNO]^+$ (100).

(OEP)Os(CO)(Et$_2$N^{15}NO). IR (KBr, cm^{-1}): ν^{15}_{NO} 1256 m, $\nu_{N^{15}N}$ 1219 m.

Preparation of [(OEP)Os(NO)(Et$_2$NNO)]BF$_4$. To a CH_2Cl_2 solution of (OEP)Os(CO)(Et_2NNO) (0.114 g, 0.133 mmol) was added $NOBF_4$ (0.016 g, 0.14 mmol). The solution turned from dark red to bright red. The solution was stirred for 30 min, and the solvent was removed. The residue was dissolved in $CDCl_3$, and a ^1H NMR spectrum was recorded. The $[(OEP)Os(NO)(Et_2NNO)]BF_4$ product was shown to be formed in quantitative yield by ^1H NMR spectroscopy. IR (KBr, cm^{-1}): ν_{NO} 1800 s, ν_{NO} (Et_2NNO) 1241 m, ν_{NN} (Et_2NNO) 1197 m; also 2969 w, 2935 w, 2874 w, 1501 m, 1469 m, 1455 m, 1435 m, 1376 m, 1317 w, 1272 m, 1241 m, 1197 m, 1155 m, 1110 m, 1056 s (possible BF_4 band), 1021 m, 996 m, 965 m, 851 m, 832 w, 749 m, 732 w, 716 m, 684 m, 625 w, 520 w. ^1H NMR ($CDCl_3$): δ 10.51 (s, 4H, pyrrole H of OEP), 4.22 (q, $J = 8$, 16H, CH_2CH_3 of OEP), 1.99 (t, $J = 8$, 24H, CH_2CH_3 of OEP), 1.99 (q, 2H, CH_3CH_2NNO, overlapping with OEP), 0.58 (q, $J = 7$, 2H, CH_3CH_2NNO), −0.52 (t, $J = 7$, 3H, CH_3CH_2NNO), −2.01 (t, $J = 7$, 3H, CH_3CH_2NNO). Low-resolution mass spectrum (FAB): *m*/*z* 855 $[(OEP)Os(NO)(Et_2NNO)]^+$ (2), 753 $[(OEP)Os(NO)]^+$ (14), 723 $[(OEP)Os]^+$ (5). Low-resolution mass spectrum (70 eV EI): *m*/*z* 102 $[Et_2NNO]^+$ (100).

Solid-State Structural Determinations. Details of crystal data and refinement are given in Table 1. The crystal data for $[(TPP)Fe(Et_2NNO)_2]ClO_4$ were collected on an Enraf Nonius CAD-4 diffractometer, and crystal data for the other four compounds were collected on a Siemens P4 diffractometer. Mo Kα ($\lambda = 0.710\,73$ Å) radiation was used in each case. The temperature for each data collection is listed in Table 1. For each case, the data were corrected for Lorentz and polarization effects. Absorption correction was applied only for (TTP)Os(CO)(Et_2NNO), and for the other four sets of crystal data it was judged to be insignificant. The SHELXTL (Siemens) system was used for structure solution, refinement, and table generation.

(i) [(TPP)Fe(THF)$_2$]ClO$_4$·2THF. The asymmetric unit contains the cation, the perchlorate anion, and two disordered THF solvent molecules. For one of the THF molecules, disorder involves only one carbon atom (C54), and it was resolved for two sites (C54A and C54B). The second THF molecule is highly disordered at several sites and did not yield a suitable model. Finally, 10 atomic positions at a partial occupancy of 0.5 were refined as carbon atoms (because of the extreme disorder, it was not possible to clearly establish the positions of the oxygen atoms). Hydrogen atoms in the idealized positions were added only for the cation. Geometrical restraints (SAME) were applied to the two bonded THF and one of the solvent THF (C53, C54B, C54A, C55, C56, O7) molecules for improving the refinement of these fragments.

(ii) [(TPP)Fe(Et$_2$NNO)$_2$]ClO$_4$. Data quality was poor because of crystal quality, and there appears to be some disorder of the perchlorate ion. Fe, Cl, and O atoms were refined anisotropically, and all of the other non-hydrogen atoms were refined isotropically. Hydrogen atoms were included in the idealized positions with a fixed isotropic temperature factor. The cation has a crystallographically imposed center of symmetry, with the Fe atom situated at that center of symmetry. The asymmetric unit contains two independent halves of the cations in special positions and the perchlorate anion in a general position.

(iii) [(OEP)Ru(NO)(H$_2$O)]BF$_4$·H$_2$O. The cation is situated at the crystallographic center of symmetry, and only half of the cation is unique. As a consequence, the N1 and O2 atoms are disordered at the same site and were refined with 50% occupancy with identical positional and thermal parameters. There is also a disordered $BF_4 \cdot H_2O$ group located in a general position, and the refinement of the occupancy factor of these atoms suggests only 50% occupancy. Hence the cation to anion ratio is 1:1. Because of the disorder of the $BF_4 \cdot H_2O$ group, the geometry is poor and displays high thermal parameters.

(iv) (OEP)Ru(CO)(Et$_2$NNO). Intensity statistics suggested the noncentric P_n space group, and the subsequent satisfactory refinement confirmed the choice of space group to be correct. The asymmetric

Table 1. Crystal Data and Structure Refinement

	[(TPP)Fe(THF)$_2$]ClO$_4$·2THF	[(TPP)Fe(Et$_2$NNO)$_2$]ClO$_4$	[(OEP)Ru(NO)(H$_2$O)]BF$_4$·H$_2$O	(OEP)Ru(CO)(Et$_2$NNO)	(TTP)Os(CO)(Et$_2$NNO)·0.5CH$_2$Cl$_2$
formula (fw)	$C_{60}H_{60}ClN_4O_8Fe$ (1056.42)	$C_{52}H_{48}ClN_8O_6Fe$ (972.28)	$C_{36}H_{48}BF_4N_5O_3Ru$ (786.67)	$C_{41}H_{54}N_6O_2Ru$ (763.97)	$C_{53.5}H_{47}ClN_6O_2Os$ (1031.6)
T, K	218(2)	183(2)	213(2)	243(2)	188(2)
cryst syst, space group	triclinic, $P\bar{1}$	monoclinic, $P2(1)/a$	monoclinic, $P2(1)/c$	monoclinic, P_n	monoclinic, $P2(1)/n$
unit cell dimens	$a = 10.756(2)$ Å $b = 13.374(3)$ Å $c = 18.706(4)$ Å $\alpha = 78.14(3)°$ $\beta = 86.61(3)°$ $\gamma = 82.18(3)°$	$a = 13.193(5)$ Å $b = 13.479(3)$ Å $c = 26.039(3)$ Å $\alpha = 90°$ $\beta = 94.39(3)°$ $\gamma = 90°$	$a = 8.423(2)$ Å $b = 22.530(5)$ Å $c = 10.678(2)$ Å $\alpha = 90°$ $\beta = 92.65(3)°$ $\gamma = 90°$	$a = 8.315(2)$ Å $b = 10.411(2)$ Å $c = 22.722(5)$ Å $\alpha = 90°$ $\beta = 90.51(3)°$ $\gamma = 90°$	$a = 9.970(2)$ Å $b = 24.386(4)$ Å $c = 19.729(3)$ Å $\alpha = 90°$ $\beta = 92.45(1)°$ $\gamma = 90°$
V, Z	2607.6(9) Å^3, 2	4617(2) Å^3, 4	2024.2(8) Å^3, 2	1966.9(7) Å^3, 2	4792.3(14) Å^3, 4
D_{calcd} (g/cm^3), cryst size (mm)	1.345, 0.26 × 0.36 × 0.42	1.399, 0.3 × 0.3 × 0.1	1.291, 0.2 × 0.4 × 0.5	1.290, 0.12 × 0.18 × 0.48	1.431, 0.54 × 0.42 × 0.36
abs coeff, mm^{-1}	0.401	0.446	0.444	0.440	2.763
F(000)	1110	2028	816	804	2080
θ range for data collection	1.57−25.0 deg	1.57−22.97 deg	1.81−24.99 deg	2.15−25.06 deg	2.07−25.00 deg
index ranges	$-1 \le h \le 12$ $-18 \le k \le 15$ $-20 \le l \le 20$	$0 \le h \le 14$ $0 \le k \le 14$ $-28 \le l \le 28$	$0 \le h \le 10$ $0 \le k \le 26$ $-12 \le l \le 12$	$0 \le h \le 9$ $0 \le k \le 12$ $-27 \le l \le 27$	$0 \le h \le 11$ $0 \le k \le 29$ $-23 \le l \le 23$
reflns collected	8082	6491	3760	3672	8868
indep reflections	7616 [$R_{int} = 0.0310$]	6382 [$R_{int} = 0.0512$]	3512 [$R_{int} = 0.0318$]	3669 [$R_{int} = 0.0955$]	8370 [$R_{int} = 0.0563$]
abs correction					semiempir from ψ scans
max. and min. transm					0.9923 and 0.5853
data/restraints/params	7582/87/721	6355/0/316	3502/0/254	3665/20/452	8290/291/596
goodness-of-fit on F^2	1.033	1.129	1.058	1.034	1.129
final R indices [$I > 2\sigma(I)$][a,b]	R1 = 0.0528, wR2 = 0.1316	R1 = 0.0668, wR2 = 0.1722	R1 = 0.0635, wR2 = 0.1597	R1 = 0.0537, wR2 = 0.1038	R1 = 0.0557, wR2 = 0.1367
R indices (all data)[a,b]	R1 = 0.0878, wR2 = 0.1754	R1 = 0.2196, wR2 = 0.2523	R1 = 0.1117, wR2 = 0.2111	R1 = 0.0818, wR2 = 0.1187	R1 = 0.0867, wR2 = 0.1954
largest diff peak and hole	0.436 and −0.330 e Å^{-3}	0.792 and −0.520 e Å^{-3}	0.676 and −0.487 e Å^{-3}	0.350 and −0.494 e Å^{-3}	1.483 and −0.782 e Å^{-3}

[a] $R1 = \sum||F_o| - |F_c||/\sum|F_o|$. [b] $wR2 = \{\sum[w(F_o^2 - F_c^2)^2]/\sum[wF_o^4]\}^{1/2}$.

unit contains one (OEP)Ru(CO)(Et_2NNO) molecule. All of the non-hydrogen atoms were refined anisotropically using the full-matrix least-squares method. Hydrogen atoms were included with idealized parameters. The carbon atoms of the Et_2NNO group display high thermal motions, suggesting a slight disorder of that group. Anisotropic displacement parameter restraint (ISOR) was applied to C2, C10, and C13 atoms for improving the displacement parameters of these atoms.

(v) (TTP)Os(CO)(Et_2NNO)·0.5CH_2Cl_2. The asymmetric unit contains one (TTP)Os(CO)(Et_2NNO) molecule and a disordered molecule of dichloromethane solvent (one of the Cl atoms of the CH_2Cl_2 molecule is disordered at two sites). The refinement of the occupancy factor of the CH_2Cl_2 atoms suggests only 50% occupancy of that molecule. All of the non-hydrogen atoms were refined anisotropically using the full-matrix least-squares method. Hydrogen atoms were included with idealized parameters only for the (TTP)Os(CO)(Et_2NNO) molecule. The Et_2NNO group is disordered, as indicated by the high thermal motion of the atoms involving this group. Geometric restraints (FLAT, SAME, and SADI) were applied to the four tolyl groups, the four pyrrole rings, and the disordered CH_2Cl_2 solvent molecule for improving the refinement of these fragments.

Results and Discussion

Iron Complexes. Reaction of (TPP)FeCl with $AgClO_4$ in hot THF for 5 min results in the formation of [(TPP)Fe($THF)_2$]ClO_4, which is isolated by filtration, addition of hexane to the filtrate, and cooling of the resulting mixture at −22 °C overnight (eq 1).

$$(TPP)FeCl + AgClO_4 \xrightarrow{THF} [(TPP)Fe(THF)_2]ClO_4 + AgCl\downarrow \quad (1)$$

Application of vacuum to solid [(TPP)Fe($THF)_2$]ClO_4 transforms it to the crystallographically characterized (TPP)Fe($OClO_3$) compound.[46] The IR spectrum (KBr) of [(TPP)Fe($THF)_2$]ClO_4 shows bands characteristic of the uncoordinated perchlorate anion at 1094 and 622 cm^{-1},[47] and it also shows bands due to the TPP macrocycle.[48] The μ_{eff} of 5.4 for this complex in C_6D_6 was measured at room temperature by the Evans method,[44] and suggests a high-spin d^5 Fe^{III} center in solution. The molecular structure of the cation of [(TPP)Fe($THF)_2$]ClO_4 is shown in Figure 1, and selected bond lengths and angles are listed in Table 2. The average Fe−N(por) bond length is 2.016(3) Å and is close to the average Fe−N(por) bond length of 2.040(9) Å in the related cation of [(TPP)Fe($THF)_2$]-{[(TPP)Fe(THF)][Cu($MNT)_2$]}·2THF.[49] However, it is slightly longer than the Fe−N(por) distance in [(OEP)Fe($THF)_2$]ClO_4 (1.999(2) Å), which is perhaps best described as an intermediate-spin Fe^{III} derivative.[50] The axial Fe−O(THF) bond lengths are 2.182(3) and 2.135(3) Å (Table 2).[51] The coordinated THF molecules are mutually perpendicular, and they are oriented between the porphyrin nitrogens (Figure 1b). The porphyrin ring exhibits a saddle distortion (Figure 1c). The related [(TPP)Fe($THF)_2$]SbF_6 compound is similarly prepared in 88% yield. Its IR spectrum (KBr) shows the presence of the uncoordinated SbF_6 anion at 656 cm^{-1}, and its μ_{eff} of 5.8 is suggestive of a high-spin Fe^{III} formulation in solution at room temperature.

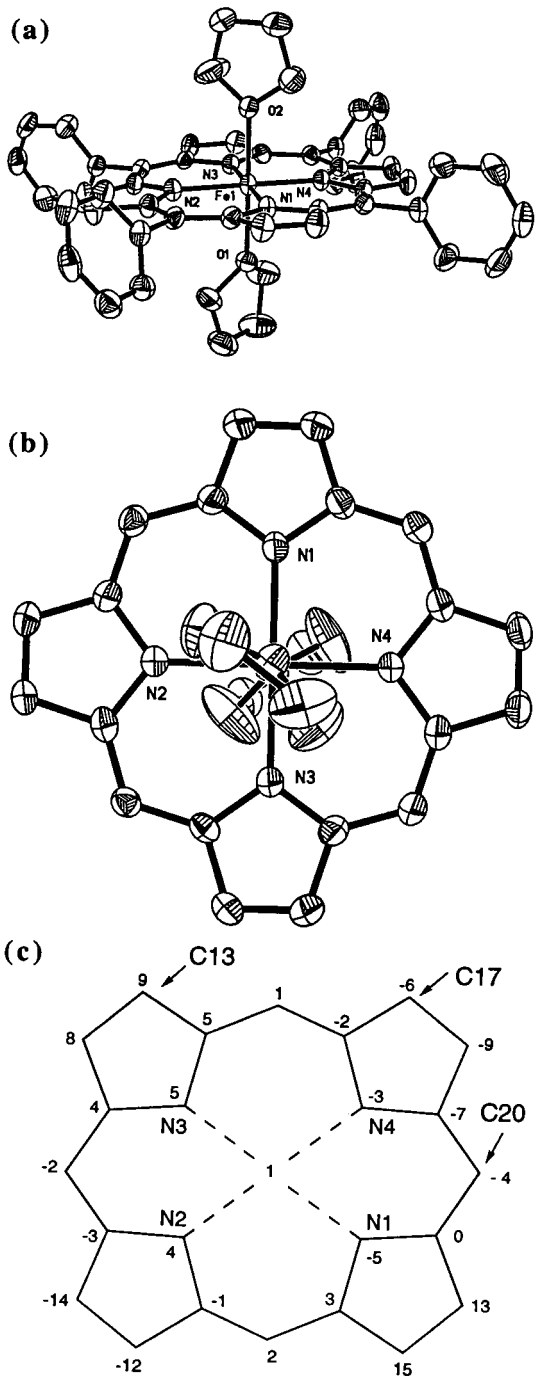

Figure 1. (a) Structure of the cation of [(TPP)Fe($THF)_2$]ClO_4. Hydrogen atoms have been omitted for clarity. (b) View of the THF orientation relative to the porphyrin core, with the view along the O−Fe bond. (c) Perpendicular atom displacements (in units of 0.01 Å) of the porphyrin core from the 24-atom mean porphyrin plane.

Diethylnitrosamine displaces the THF ligands in [(TPP)Fe($THF)_2$]ClO_4 in toluene to give the [(TPP)Fe($Et_2NNO)_2$]ClO_4 bis-nitrosamine product (eq 2).

$$[(TPP)Fe(THF)_2]ClO_4 + \text{excess } Et_2NNO \rightarrow [(TPP)Fe(Et_2NNO)_2]ClO_4 + 2THF \quad (2)$$

This product is isolated in analytically pure form in 96% yield as a dark purple microcrystalline solid. The IR spectrum (KBr)

(46) Reed, C. A.; Mashiko, T.; Bentley, S. P.; Kastner, M. E.; Scheidt, W. R.; Spartalian, K.; Lang, G. *J. Am. Chem. Soc.* **1979**, *101*, 2948−2958.
(47) Gowda, N. M. N.; Naikar, S. B.; Reddy, G. K. N. *Adv. Inorg. Chem. Radiochem.* **1984**, *28*, 255.
(48) Kitagawa, T.; Ozaki, Y. *Struct. Bonding* **1987**, *64*, 71−114.
(49) Serr, B. R.; Headford, C. E. L.; Anderson, O. P.; Elliot, C. M.; Spartalian, K.; Fainzilberg, V. E.; Hatfield, W. E.; Rohrs, B. R.; Eaton, S. S.; Eaton, G. R. *Inorg. Chem.* **1992**, *31*, 5450−5465.
(50) Cheng, B.; Safo, M. K.; Orosz, R. D.; Reed, C. A.; Debrunner, P. G.; Scheidt, W. R. *Inorg. Chem.* **1994**, *33*, 1319−1324.
(51) Other structurally characterized six-coordinate (refs 52−57) and five-coordinate [(por)Fe(O-donor)$_n$]$^{m+}$ complexes (refs 49, 50, and 58) have been reported.

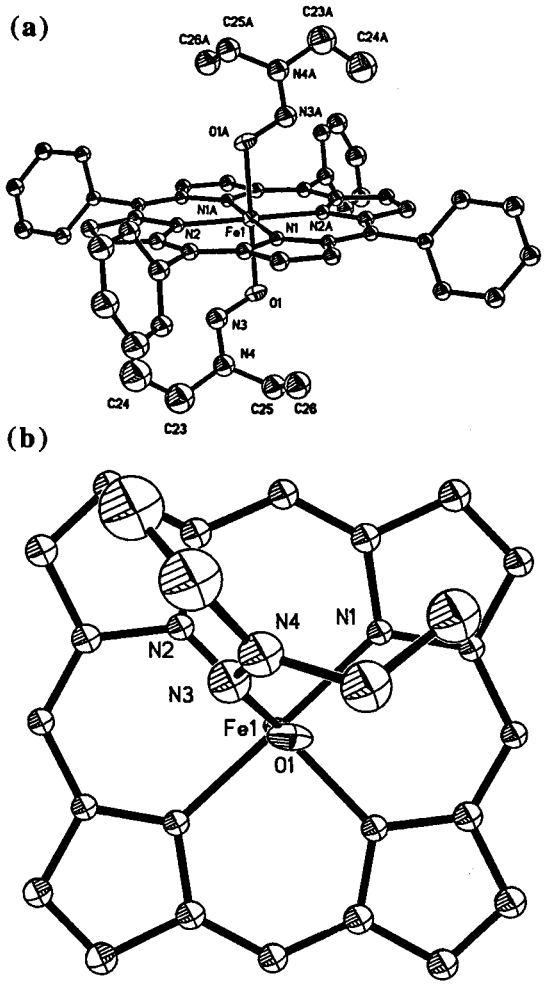

Figure 2. (a) Structure of one of the cations (cation 1) of [(TPP)Fe-$(Et_2NNO)_2]ClO_4$. Hydrogen atoms have been omitted for clarity. (b) View of the nitrosamine orientation relative to the porphyrin core, with the view along the O(1)−Fe(1) bond.

Table 2. Selected Bond Lengths and Angles for $[(TPP)Fe(THF)_2]ClO_4 \cdot 2THF$

Bond Lengths (Å)			
Fe(1)−N(1)	2.021(3)	Fe(1)−N(4)	2.012(3)
Fe(1)−N(2)	2.014(3)	Fe(1)−O(1)	2.182(3)
Fe(1)−N(3)	2.017(3)	Fe(1)−O(2)	2.135(3)
Bond Angles (deg)			
O(1)−Fe(1)−O(2)	178.76(11)	N(3)−Fe(1)−O(1)	87.90(12)
N(1)−Fe(1)−O(1)	91.52(12)	N(3)−Fe(1)−O(2)	90.86(12)
N(1)−Fe(1)−O(2)	89.72(12)	N(4)−Fe(1)−O(1)	89.96(12)
N(2)−Fe(1)−O(1)	89.71(12)	N(4)−Fe(1)−O(2)	90.10(12)
N(2)−Fe(1)−O(2)	90.24(12)		

shows a new band at 1270 cm^{-1} attributed to ν_{NO} and ν_{NN} (as overlapping bands) of the coordinated Et_2NNO ligands. The use of $Et_2N^{15}NO$ (i.e., nitroso ^{15}N-labeled) in this reaction shifts this band to 1254 cm^{-1} ($\Delta\nu$ = 16 cm^{-1}). Free aliphatic secondary nitrosamines generally display ν_{NO}'s in the 1460−1425 cm^{-1} region and ν_{NN}'s in the 1150−1030 cm^{-1} region.[59] The μ_{eff} of 5.9 (C_6D_6) is indicative of a high-spin Fe^{III}

Table 3. Selected Bond Lengths and Angles for $[(TPP)Fe(Et_2NNO)_2]ClO_4$

Bond Lengths (Å)			
Fe(1)−N(1)	2.042(6)	Fe(2)−N(5)	2.032(6)
Fe(1)−N(2)	2.046(6)	Fe(2)−N(6)	2.044(7)
Fe(1)−O(1)	2.107(6)	Fe(2)−O(2)	2.104(5)
O(1)−N(3)	1.260(9)	O(2)−N(7)	1.285(8)
N(3)−N(4)	1.276(10)	N(7)−N(8)	1.288(9)
N(4)−C(23)	1.468(12)	N(8)−C(49)	1.475(11)
N(4)−C(25)	1.442(12)	N(8)−C(51)	1.457(10)
C(23)−C(24)	1.45(2)	C(49)−C(50)	1.500(12)
C(25)−C(26)	1.527(14)	C(51)−C(52)	1.559(13)
Bond Angles (deg)			
N(1)−Fe(1)−O(1)	87.1(2)	N(5)−Fe(2)−O(2)	89.6(2)
N(2)−Fe(1)−O(1)	92.9(2)	N(6)−Fe(2)−O(2)	87.1(2)
N(3)−O(1)−Fe(1)	116.3(5)	N(7)−O(2)−Fe(2)	114.8(5)
O(1)−N(3)−N(4)	113.9(7)	O(2)−N(7)−N(8)	113.6(7)
N(3)−N(4)−C(25)	122.8(8)	N(7)−N(8)−C(49)	123.4(7)
N(3)−N(4)−C(23)	117.0(8)	N(7)−N(8)−C(51)	115.3(7)
C(23)−N(4)−C(25)	120.1(8)	C(49)−N(8)−C(51)	121.3(7)
N(4)−C(23)−C(24)	115.0(10)	N(8)−C(49)−C(50)	113.6(8)
N(4)−C(25)−C(26)	112.0(8)	N(8)−C(51)−C(52)	110.0(7)

formulation for the nitrosamine complex in solution. The solid-state structure of the cation of $[(TPP)Fe(Et_2NNO)_2]ClO_4$ is shown in Figure 2, with selected bond lengths and angles listed in Table 3. The orientation of the two independent cations with respect to the perchlorate anion is displayed in Figure 3, and the two porphyrin planes are oriented 66.8° to each other. The average Fe−N(por) bond length is 2.041 Å, and the average Fe−O(axial) bond length is 2.106 Å. These data are consistent with a high-spin Fe^{III} formulation for this complex.[60] The most interesting feature of the structure is that the nitrosamine ligands are bound to the formally Fe^{III} center in a η^1-O fashion. The average nitrosamine O−N and N−N bond lengths are 1.272 and 1.282 Å, respectively. The Fe−O−N(nitrosamine) and O−N−N bond angles are 115.6° (average) and 113.8° (average), respectively. The nitrosamine $ONNC_2$ fragments are essentially planar. The structure of free diethylnitrosamine has not been reported. However, the structural data for the complexed nitrosamine in $[(TPP)Fe(Et_2NNO)_2]ClO_4$ may be compared to related distances in free dimethylnitrosamine of 1.234 Å (N−O) and 1.344 Å (N−N) as determined by electron diffraction,[61] and 1.260(6) Å (N−O) and 1.320(6) Å (N−N) as determined by low-temperature X-ray diffraction.[62] The complexed diethylnitrosamine is best represented by a resonance hybrid having a significant contribution from structure **B**.

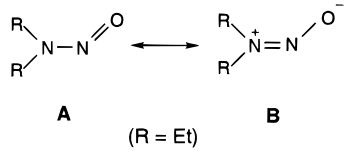

A similar contribution from the dipolar structure **B** (R = Me) is noted in the low-temperature X-ray structure of dimethylnitrosamine.[62] The O(1)−N(3)-N(4)−C(25) and O(1)−N(3)-N(4)−C(23) torsion angles in cation 1 are 1.11° and 177.81°,

(52) Scheidt, W. R.; Geiger, D. K.; Lee, Y. J.; Gans, P.; Marchon, J.-C. *Inorg. Chem.* **1992**, *31*, 2660−2663.
(53) Scheidt, W. R.; Cohen, I. A.; Kastner, M. E. *Biochemistry* **1979**, *18*, 3546−3552.
(54) Mashiko, T.; Kastner, M. E.; Spartalian, K.; Scheidt, W. R.; Reed, C. A. *J. Am. Chem. Soc.* **1978**, *100*, 6354−6362.
(55) Senge, M. O. *Acta Crystallogr.* **1996**, *C52*, 302−305.
(56) Einstein, F. W. B.; Willis, A. C. *Inorg. Chem.* **1978**, *17*, 3040−3045.
(57) Reed, C. A.; Mashiko, T.; Scheidt, W. R.; Spartalian, K.; Lang, G. *J. Am. Chem. Soc.* **1980**, *102*, 2302−2306.
(58) Kellet, P. J.; Pawlik, M. J.; Taylor, L. F.; Thompson, R. G.; Levstik, M. A.; Anderson, O. P.; Strauss, S. H. *Inorg. Chem.* **1989**, *28*, 440−447.
(59) Williams, R. L.; Pace, R. J.; Jeacocke, G. J. *Spectrochim. Acta* **1964**, *20*, 225−236.
(60) Scheidt, W. R.; Reed, C. A. *Chem. Rev.* **1981**, *81*, 543−555.
(61) Rademacher, P.; Stølevik, R. *Acta Chem. Scand.* **1969**, *23*, 660−671.
(62) Krebs, B.; Mandt, J. *Chem. Ber.* **1975**, *108*, 1130−1137.

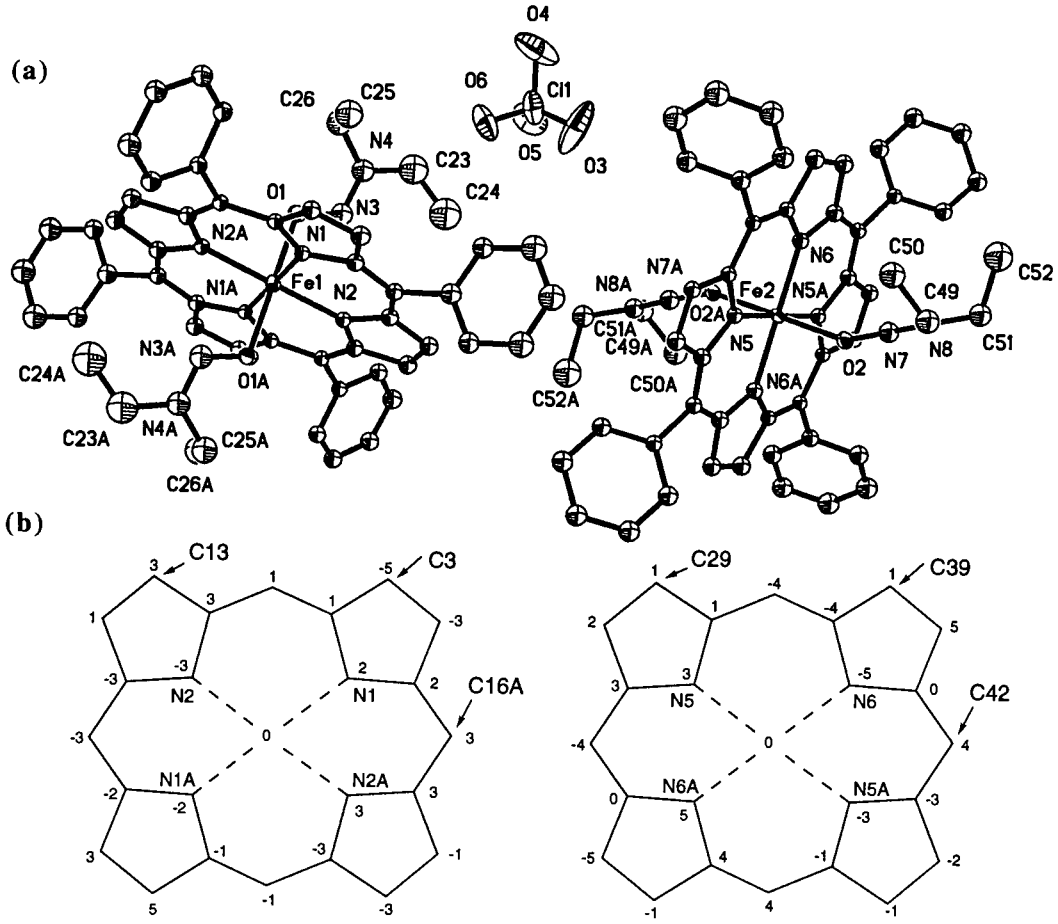

Figure 3. (a) View of the two cations of $[(TPP)Fe(Et_2NNO)_2]ClO_4$, showing their orientation with respect to the perchlorate anion. (b) Perpendicular atom displacements (in units of 0.01 Å) of the two porphyrin cores (cation 1 on the left, and cation 2 on the right) from their 24-atom mean porphyrin planes. The O(1) and O(2) atoms project outward toward the reader.

respectively, with a mean deviation of 0.010 Å from the $ONNC_2$ plane. The analogous O(2)−N(7)−N(8)−C(51) and O(2)−N(7)−N(8)−C(49) torsion angles in cation 2 are 178.73 and −2.27°, respectively, with a mean deviation of 0.007 Å from the $ONNC_2$ plane. The nitrosamine ligand in cation 1 essentially eclipses a porphyrin nitrogen (Figure 2b), with a N(2)−Fe(1)−O(1)−N(3) torsion angle of 3.8°. However, the related N(5A)-Fe(2)−O(2)−N(7) torsion angle in cation 2 is 19.65°.

Prior to this work the only other structurally characterized transition metal complex with discrete nitrosamine ligands was $((CH_3)_2NNO)CuCl_2$ with N−O and N−N distances of 1.22(2) and 1.29(2) Å, respectively.[15] Recently, the related structure of $((CH_2)_5NNO)CuCl_2$ was also reported.[12] Although the structures of these Cu complexes reveal a dominant nitrosamine−metal interaction via the nitroso O atom, the nitroso N atom is also found to interact with the metal. Thus, the structure of $[(TPP)Fe(Et_2NNO)_2]ClO_4$ represents the first unambiguous determination of a sole η^1-O binding mode for nitrosamines in transition metal complexes. Structures of palladium and platinum complexes with C,N-bonded nitrosamines are known.[36,37]

The related tetratolylporphyrin complex, $[(TTP)Fe(Et_2NNO)_2]SbF_6$, is also preparable in 70% yield by the reaction of the precursor bis-THF compound with excess diethylnitrosamine. The ν_{NO} and ν_{NN} bands are distinguishable in the IR spectrum of this complex, appearing at 1271 and 1256 cm^{-1}, respectively. The IR spectrum also shows a band at 657 cm^{-1} due to the uncoordinated SbF_6 anion, and the μ_{eff} of 6.0 (C_6D_6) suggests a high-spin Fe^{III} spin state in solution. The synthesis of metalloporphyrin nitrosamine complexes has also been extended to the formation of the air-sensitive thionitrosamine complex, $[(TPP)Fe(Me_2NNS)_2]ClO_4$, as outlined in the Experimental Section. The IR spectrum (KBr) of this complex shows bands due to the coordinated thionitrosamines at 1393 m, 1373 m, 1120 s, 766 s, and 711 m cm^{-1}, with the bands at 1120 and 766 cm^{-1} being assigned to ν_{NN} and ν_{NS}, respectively, of the bound dimethylthionitrosamine. The ν_{NN} and ν_{NS} bands of coordinated S-bound dimethylthionitrosamines generally occur in the 1125−1135 and 770−782 cm^{-1} ranges, respectively.[63−68] In particular, the shift of ν_{NN} of 15 cm^{-1} to higher wavenumbers, and the shift of ν_{NS} of 144 cm^{-1} to lower wavenumbers from those of the free ligand (at 1105 cm^{-1} for ν_{NN}, and 910 cm^{-1} for ν_{NS})[63] is consistent with a contribution of the dipolar $^-S-N{=}N^+Me_2$ form in the iron porphyrin complex (as seen in the nitrosamine analogue discussed earlier). Molecular structures of other metal complexes of thionitrosamines are known,[63,68−70] and these reveal S-binding of the R_2NNS ligands.

(63) Tresoldi, G.; Bruno, G.; Piraino, P.; Faraone, G.; Bombieri, G. *J. Organomet. Chem.* **1984**, *265*, 311−322.
(64) Herberhold, M.; Hill, A. F. *J. Organomet. Chem.* **1986**, *315*, 105−112.
(65) Tresoldi, G.; Sergi, S.; Schiavo, S. L.; Piraino, P. *J. Organomet. Chem.* **1987**, *322*, 369−376.
(66) Tresoldi, G.; Sergi, S.; Schiavo, S. L.; Piraino, P. *J. Organomet. Chem.* **1987**, *328*, 387−391.
(67) Tresoldi, G.; Bruno, G.; Crucitti, F.; Piraino, P. *J. Organomet. Chem.* **1983**, *252*, 381−387.
(68) Roesky, H. W.; Emmert, R.; Isenberg, W.; Schmidt, M.; Sheldrick, G. M. *J. Chem. Soc., Dalton Trans.* **1983**, 183−185.

However, we have not yet been able to prepare suitable crystals of $[(TPP)Fe(Me_2NNS)_2]ClO_4$ for X-ray diffraction studies.

We then sought to prepare the related Fe^{II} nitrosamine complexes to investigate the nature of nitrosamine binding to the metal centers. In particular, we envisioned that if we could prepare a complex of the form $[(por)Fe(NO)(Et_2NNO)]^+$, then the linear NO ligand (regarded formally as NO^+) would formally provide the required Fe^{II} center. Indeed, reaction of $[(TPP)Fe(Et_2NNO)_2]ClO_4$ with NO gas results in the formation of a dark-purple microcrystalline product formulated as the nitrosyl nitrosamine $[(TPP)Fe(NO)(Et_2NNO)]ClO_4$ complex on the basis of its IR spectrum. Thus, a new band at 1916 cm^{-1} is attributed to the unique ν_{NO} band of the Fe−NO fragment, whereas the 1268 cm^{-1} band is attributed to the ν_{NO} and ν_{NN} bands (overlapped) of the nitrosamine fragment. Notably, this 1268 cm^{-1} band is now reduced in intensity (as expected) by about half from that of the parent bis-nitrosamine $[(TPP)Fe(Et_2NNO)_2]ClO_4$ complex. The similarity of the IR spectra of the two complexes suggests that the η^1-O binding mode of the nitrosamine is not altered in the nitrosyl derivative. Unfortunately, this nitrosyl nitrosamine product is thermally unstable, and we have not been able to isolate it in pure form.

We then proceeded to prepare the analogous Ru^{II} complex, namely, $[(por)Ru(NO)(Et_2NNO)]^+$, in an attempt to generate a more thermally stable (and perhaps isolable) complex.

Ruthenium Complexes. We have previously shown that the reaction of (TPP)Ru(CO) with the nitrosonium cation followed by isolation in air produces $[(TPP)Ru(NO)(H_2O)]^+$.[71]

IR monitoring of the reaction of (OEP)Ru(CO) with $NOBF_4$ in CH_2Cl_2 reveals the replacement of the ν_{CO} band of (OEP)Ru(CO) at 1919 cm^{-1} with a band at 1878 cm^{-1} assigned to ν_{NO} of the $[(OEP)Ru(NO)]^+$ cation. Our attempts to isolate this cation were not successful. However, the aqua derivative forms when the reaction solution is exposed to air, and the $[(OEP)Ru(NO)(H_2O)]^+$ product is isolable from the reaction mixture as dark purple crystals in 71% yield (eq 3). The ν_{NO} of 1852

$$(OEP)Ru(CO) + NOBF_4 \xrightarrow[\text{(ii) air}]{\text{(i) } CH_2Cl_2} [(OEP)Ru(NO)(H_2O)]BF_4 + CO \quad (3)$$

cm^{-1} (KBr) in the IR spectrum of $[(OEP)Ru(NO)(H_2O)]BF_4$ is indicative of a linear terminal nitrosyl ligand. The linearity of the terminal NO ligand was confirmed by a single-crystal X-ray crystallographic analysis of the compound. The structure is shown in Figure 4, and selected bond lengths and angles are listed in Table 4. The Ru−N(por) bond lengths are 2.044(5) and 2.039(5) Å, and these lie within the 1.88(2)−2.10(3) Å range[72] observed for other crystallographically characterized $(OEP)Ru^{II}$ porphyrins.[73−82] The nitrosyl and aqua ligands are disordered over the two axial sites, limiting the accuracy of the bond lengths and angles involving these groups. The BF_4 anion

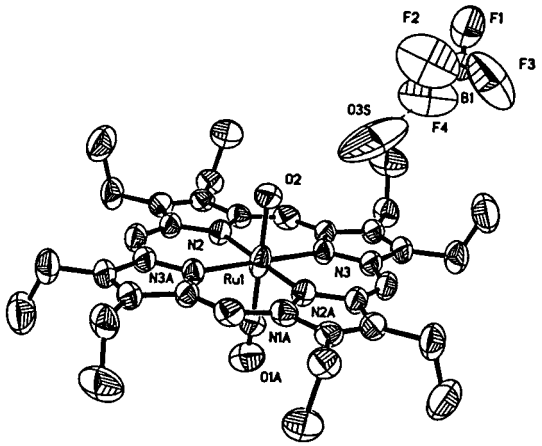

Figure 4. Structure of $[(OEP)Ru(NO)(H_2O)]BF_4 \cdot H_2O$. Hydrogen atoms have been omitted for clarity.

Table 4. Selected Bond Lengths and Angles for $[(OEP)Ru(NO)(H_2O)]BF_4 \cdot H_2O$[a]

Bond Lengths (Å)			
Ru(1)−O(2)	1.888(5)	O(3S)-F(4)	2.261(40)
Ru(1)−N(1)	1.888(5)	O(3S)-F(2)	2.498(34)
Ru(1)−N(2)	2.044(5)	O(3S)-O(1)	2.849(35)
Ru(1)−N(3)	2.039(5)	O(3S)-O(2)	3.172(34)
N(1)−O(1)	1.138(12)		

Bond Angles (deg)			
Ru(1)−N(1)−O(1)	171.0(7)	N(1)−Ru(1)−N(2)	91.4(2)
O(2)−Ru(1)−N(2)	91.4(2)	N(1)−Ru(1)−N(3)	90.8(2)
O(2)−Ru(1)−N(3)	90.8(2)	N(2)−Ru(1)−N(3)	90.5(2)

[a] The nitrosyl and water ligands are disordered over the two sites.

is hydrogen-bonded to the second water molecule, with the closest fluorine−oxygen distance being 2.26(4) Å.

Diethylnitrosamine displaces the aqua ligand in $[(OEP)Ru(NO)(H_2O)]^+$ to give the air-stable $[(OEP)Ru(NO)(Et_2NNO)]^+$ derivative in 82% yield (eq 4).

$$[(OEP)Ru(NO)(H_2O)]BF_4 + Et_2NNO \rightarrow [(OEP)Ru(NO)(Et_2NNO)]BF_4 + H_2O \quad (4)$$

The ^1H NMR spectrum of the formally Ru^{II} d^6 diamagnetic $[(OEP)Ru(NO)(Et_2NNO)]^+$ complex shows peaks due to the OEP macrocycle as well as peaks at 1.94 and 0.58 ppm (as quartets for CH_2CH_3) and at −0.50 and −1.98 ppm (as triplets for CH_2CH_3) due to the coordinated nitrosamine. These latter peaks are shifted upfield by 2−3 ppm from those of free Et_2NNO, consistent with the coordination of the nitrosamine fragment to the ruthenium center.

The ν_{NO} of the unique nitrosyl Ru−NO fragment of $[(OEP)Ru(NO)(Et_2NNO)]^+$ is at 1847 cm^{-1}, shifted by 5 cm^{-1} to lower wavenumbers from that of the aqua precursor. New

(69) Roesky, H. W.; Emmert, R.; Clegg, W.; Isenberg, W.; Sheldrick, G. M. *Angew. Chem., Int. Ed. Engl.* **1981**, *20*, 591−592.
(70) Gieren, A.; Ruiz-Pérez, C.; Hübner, T.; Herberhold, M.; Hill, A. F. *J. Chem. Soc., Dalton Trans.* **1988**, 1693−1696.
(71) Kadish, K. M.; Adamian, V. A.; Caemelbecke, E. V.; Tan, Z.; Tagliatesta, P.; Bianco, P.; Boschi, T.; Yi, G.-B.; Khan, M. A.; Richter-Addo, G. B. *Inorg. Chem.* **1996**, *35*, 1343−1348.
(72) Slebodnick, C.; Seok, W. K.; Kim, K.; Ibers, J. A. *Inorg. Chim. Acta* **1996**, *243*, 57−65.
(73) Kadish, K. M.; Hu, Y.; Mu, X. H. *J. Heterocycl. Chem.* **1991**, *28*, 1821−1824.
(74) Funatsu, K.; Kimura, A.; Imamura, T.; Ichimura, A.; Sasaki, Y. *Inorg. Chem.* **1997**, *36*, 1625−1635.
(75) Hopf, F. R.; O'Brein, T. P.; Scheidt, W. R.; Whitten, D. G. *J. Am. Chem. Soc.* **1975**, *97*, 277−281.
(76) Ariel, S.; Dolphin, D.; Domazetis, G.; James, B. R.; Leung, T. W.; Rettig, S. J.; Trotter, J.; Williams, G. M. *Can. J. Chem.* **1984**, *62*, 755−762.
(77) Miranda, K. M.; Bu, X.; Lorkovic, I.; Ford, P. C. *Inorg. Chem.* **1997**, *36*, 4838−4848.
(78) Yi, G.-B.; Khan, M. A.; Richter-Addo, G. B. *Chem. Commun.* **1996**, 2045−2046.
(79) Yi, G.-B.; Chen, L.; Khan, M. A.; Richter-Addo, G. B. *Inorg. Chem.* **1997**, *36*, 3876−3885.
(80) Yi, G.-B.; Khan, M. A.; Powell, D. R.; Richter-Addo, G. B. *Inorg. Chem.* **1998**, *37*, 208−214.
(81) James, B. R.; Pacheco, A.; Rettig, S. J.; Ibers, J. A. *Inorg. Chem.* **1988**, *27*, 2414−2421.
(82) Yee, G. T.; Noll, B. C.; Williams, D. K. C.; Sellers, S. P. *Inorg. Chem.* **1997**, *36*, 2904−2907.

bands in the IR spectrum at 1250 and 1201 cm^{-1} are assigned to ν_{NO} and ν_{NN}, respectively, of the coordinated diethylnitrosamine. To aid in the assignments of ν_{NO} and ν_{NN} of the coordinated nitrosamine, we prepared the isotope-labeled $[(OEP)Ru(NO)(Et_2N^{15}NO)]^+$ and $[(OEP)Ru(NO)(Et_2NN^{18}O)]^+$ derivatives. The use of $Et_2N^{15}NO$ shifts the nitrosamine ν_{NO} and ν_{NN} bands of the $[(OEP)Ru(NO)(Et_2N^{15}NO)]^+$ derivative to 1234 and 1194 cm^{-1}, respectively, and the use of $Et_2NN^{18}O$ results in a shift of the original 1250 cm^{-1} band in the unlabeled $[(OEP)Ru(NO)(Et_2NNO)]^+$ complex to 1240 cm^{-1} in $[(OEP)Ru(NO)(Et_2NN^{18}O)]^+$. These isotope-labeled studies confirm the assignments of the 1250 and 1201 cm^{-1} bands in the IR spectrum of $[(OEP)Ru(NO)(Et_2NNO)]^+$ to ν_{NO} and ν_{NN}, respectively, of the coordinated nitrosamine. Although these IR spectroscopic properties are consistent with the formulation of the $[(OEP)Ru(NO)(Et_2NNO)]^+$ complex as containing an O-bonded nitrosamine similar to that in $[(TPP)Fe(Et_2NNO)_2]^+$ (vide supra), we have not yet been able to obtain a suitable crystal for X-ray diffraction studies.

Gratifyingly, we were able to obtain suitable crystals of the valence isoelectronic *carbonyl* $(OEP)Ru(CO)(Et_2NNO)$ complex, which we prepared by the direct reaction of (OEP)Ru(CO) with excess diethylnitrosamine. The IR spectrum (KBr) of $(OEP)Ru(CO)(Et_2NNO)$ reveals a ν_{CO} of 1910 cm^{-1}, with the nitrosamine ν_{NO} and ν_{NN} bands at 1301 and 1257 cm^{-1}, respectively. The use of $Et_2N^{15}NO$ shifts these latter bands to 1287 and 1248 cm^{-1}, and the use of $Et_2NN^{18}O$ results in a shift of the original 1301 cm^{-1} (ν_{NO}) band in the unlabeled complex to 1284 cm^{-1} in $(OEP)Ru(CO)(Et_2NN^{18}O)$. The larger $\Delta\nu$ (i.e., $|\nu_{NO} - \nu_{NN}|$) in the Ru^{II} nitrosamine complexes compared to the insignificant $\Delta\nu$ (for the (TPP)Fe case) or small $\Delta\nu$ (for the (TTP)Fe case) in the cationic Fe^{III} derivatives (vide supra) is suggestive of a *decreased* contribution of the dipolar resonance structure of the nitrosamine in the Ru compounds.

The molecular structure of $(OEP)Ru(CO)(Et_2NNO)$ is shown in Figure 5. Selected bond lengths and angles are collected in Table 5. The Ru−C(O) and C−O bond lengths are 1.788(9) and 1.181(10) Å, respectively, and the Ru−C−O bond angle is 177.0(7)°. The Ru−N(por) bond length is 2.049 Å (average). These data are similar to those determined for other structurally characterized (OEP)Ru(CO)-containing complexes.[73,74,83] The nitrosamine ligand is bound to the Ru^{II} center in a η^1-O fashion. The axial Ru−O(nitrosamine) distance is 2.199(6) Å and lies within the 2.123(9)−2.348(3) Å range observed for other nonnitrosyl Ru^{II} porphyrins with O-donor ligands.[73,83−90] The nitrosamine O−N and N−N bond lengths are 1.243(8) and 1.287(9) Å, respectively, and the nitrosamine O−N−N bond angle is 113.9(7)°. The nitrosamine functionality is planar, with O(2)−N(5)−N(6)−C(38) and O(2)−N(5)−N(6)−C(40) torsion angles of 0° and 178.8°, respectively. The nitrosamine ligand

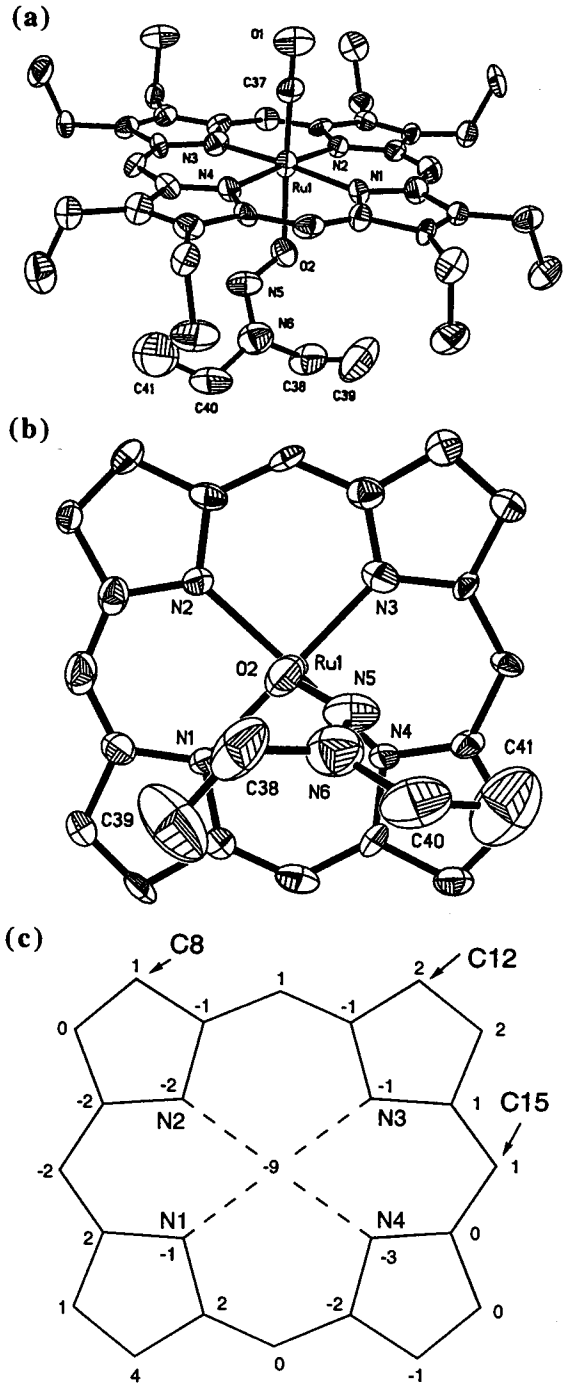

Figure 5. (a) Structure of $(OEP)Ru(CO)(Et_2NNO)$. Hydrogen atoms have been omitted for clarity. (b) View of the nitrosamine orientation relative to the porphyrin core, with the view along the O(2)−Ru(1) bond. (c) Perpendicular atom displacements (in units of 0.01 Å) of the porphyrin core from the 24-atom mean porphyrin plane.

essentially eclipses a porphyrin nitrogen (Figure 5b), with a N(4)−Ru(1)−O(2)−N(5) torsion angle of 16.9°.

Reaction of $(OEP)Ru(CO)(Et_2NNO)$ with the nitrosonium cation in CH_2Cl_2 results in the formation of the cationic nitrosyl $[(OEP)Ru(NO)(Et_2NNO)]^+$ product in quantitative yield by IR and ^1H NMR spectroscopy (eq 5).

$$(OEP)Ru(CO)(Et_2NNO) + NOBF_4 \rightarrow [(OEP)Ru(NO)(Et_2NNO)]BF_4 + CO \quad (5)$$

A similar reaction with $^{15}NOBF_4$ produces $[(OEP)Ru(^{15}NO)$-

(83) Seyler, J. W.; Fanwick, P. E.; Leidner, C. R. *Inorg. Chem.* **1992**, *31*, 3699−3700.
(84) Bonnet, J. J.; Eaton, S. S.; Eaton, G. R.; Holm, R. H.; Ibers, J. A. *J. Am. Chem. Soc.* **1973**, *95*, 2141−2149.
(85) Lo, W.-C.; Che, C.-M.; Cheng, K.-F.; Mak, T. C. W. *Chem. Commun.* **1997**, 1205−1206.
(86) Groves, J. T.; Han, Y.; Van engen, D. *J. Chem. Soc., Chem. Commun.* **1990**, 436−437.
(87) Birnbaum, E. R.; Schaefer, W. P.; Labinger, J. A.; Bercaw, J. E.; Gray, H. B. *Inorg. Chem.* **1995**, *34*, 1751−1755.
(88) Maux, P. L.; Bahri, H.; Simonneaux, G.; Toupet, L. *Inorg. Chem.* **1995**, *34*, 4691−4697.
(89) Slebodnick, C.; Kim, K.; Ibers, J. A. *Inorg. Chem.* **1993**, *32*, 5338−5342.
(90) Camenzind, M. J.; James, B. R.; Dolphin, D.; Sparapany, J. W.; Ibers, J. A. *Inorg. Chem.* **1988**, *27*, 3054−3057.

Table 5. Selected Bond Lengths and Angles for (OEP)Ru(CO)(Et_2NNO)

Bond Lengths (Å)			
Ru(1)−C(37)	1.788(9)	O(2)−N(5)	1.243(8)
C(37)−O(1)	1.181(10)	N(5)−N(6)	1.287(9)
Ru(1)−N(1)	2.059(5)	N(6)−C(38)	1.437(11)
Ru(1)−N(2)	2.042(6)	N(6)−C(40)	1.451(13)
Ru(1)−N(3)	2.034(6)	C(38)−C(39)	1.54(2)
Ru(1)−N(4)	2.060(6)	C(40)−C(41)	1.50(2)
Ru(1)−O(2)	2.199(6)		

Bond Angles (deg)			
Ru(1)−C(37)−O(1)	177.0(7)	N(5)−N(6)−C(40)	117.8(8)
C(37)−Ru(1)−O(2)	176.2(3)	C(38)−N(6)−C(40)	118.8(8)
Ru(1)−O(2)−N(5)	115.3(5)	N(6)−C(38)−C(39)	111.4(9)
O(2)−N(5)−N(6)	113.9(7)	N(6)−C(40)−C(41)	115.2(9)
N(5)−N(6)−C(38)	123.4(8)		

(Et_2NNO)]BF_4 (ν^{15}_{NO} 1808 cm^{-1}), confirming the replacement of the CO ligand with the *incoming* NO^+ electrophile.[91]

The coordinated nitrosamine in [(OEP)Ru(NO)(Et_2NNO)]$^+$ is readily displaced by diethylamine to give the nitrosyl amine [(OEP)Ru(NO)($HNEt_2$)]$^+$ complex in 71% yield (eq 6). This amine complex is also obtained in 78% yield from the direct reaction of the precursor aqua [(OEP)Ru(NO)(H_2O)]$^+$ complex with diethylamine (eq 7).

$$[(OEP)Ru(NO)(Et_2NNO)]BF_4 + HNEt_2 \rightarrow [(OEP)Ru(NO)(HNEt_2)]BF_4 + Et_2NNO \quad (6)$$

$$[(OEP)Ru(NO)(H_2O)]BF_4 + HNEt_2 \rightarrow [(OEP)Ru(NO)(HNEt_2)]BF_4 + H_2O \quad (7)$$

The IR spectrum reveals a new band at 3156 cm^{-1}, which is attributed to ν_{NH} of the coordinated amine in [(OEP)Ru(NO)-($HNEt_2$)]BF_4. The ν_{NO} of 1824 cm^{-1} (KBr) is lower than those of [(OEP)Ru(NO)(H_2O)]BF_4 (1852 cm^{-1}) and [(OEP)Ru(NO)(Et_2-NNO)]BF_4 (1847 cm^{-1}), and this suggests that the relative ordering of ligand Lewis basicity in these cationic ruthenium nitrosyl porphyrins is H_2O < Et_2NNO < $HNEt_2$.

Osmium Complexes. The (OEP)Os(CO)(Et_2NNO) compound is generated in 66% isolated yield from the reaction of (OEP)Os(CO) with excess diethylnitrosamine (eq 8). The related TTP analogue is produced similarly in 74% isolated yield.

$$(por)Os(CO) + Et_2NNO \rightarrow (por)Os(CO)(Et_2NNO) \quad (8)$$

$$por = OEP, TTP$$

These are the first osmium nitrosamine complexes to be reported.[92] The ν_{CO} of the (OEP)Os(CO)(Et_2NNO) product is at 1883 cm^{-1}, and the nitrosamine ν_{NO} and ν_{NN} bands are at 1294 and 1222 cm^{-1}, respectively. The use of $Et_2N^{15}NO$ shifts these latter bands to 1256 and 1219 cm^{-1}. The IR spectrum of the related (TTP)Os(CO)(Et_2NNO) product reveals its ν_{CO} at 1902 cm^{-1}, and the nitrosamine ν_{NO} and ν_{NN} bands at 1292 and 1251 cm^{-1}, respectively (ν^{15}_{NO} 1275 and $\nu_{N^{15}N}$ 1246 cm^{-1}).

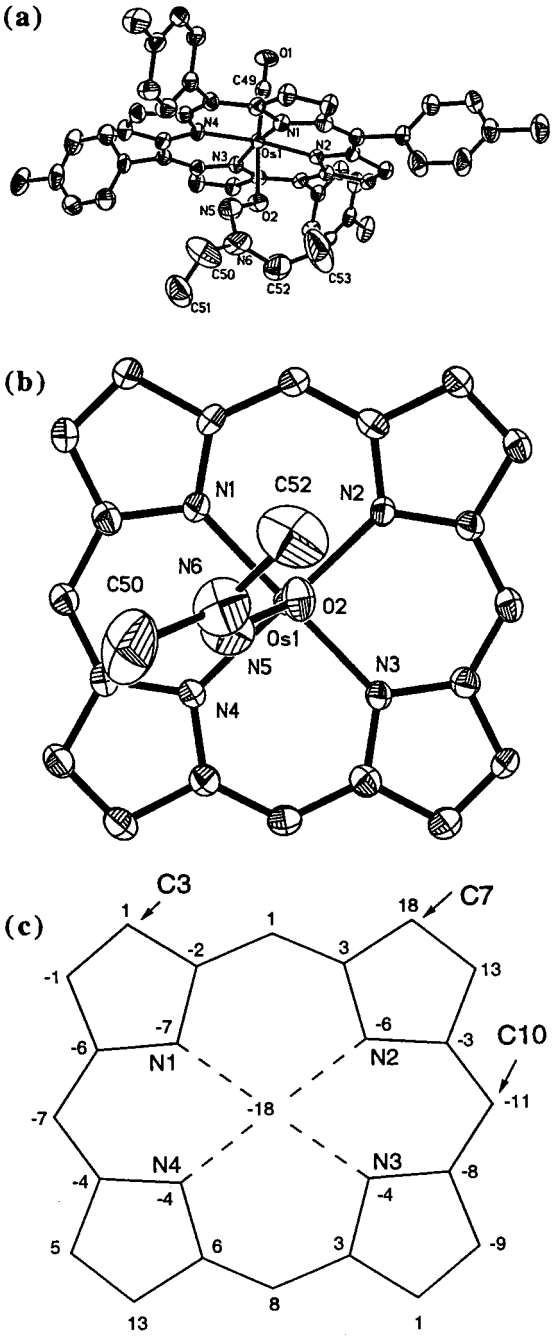

Figure 6. (a) Structure of (TTP)Os(CO)(Et_2NNO). Hydrogen atoms have been omitted for clarity. (b) View of the nitrosamine orientation relative to the porphyrin core, with the view along the O(2)−Os(1) bond. (c) Perpendicular atom displacements (in units of 0.01 Å) of the porphyrin core from the 24-atom mean porphyrin plane.

The higher ν_{CO} for the TTP analogue is consistent with the greater π acidity of the TTP ring compared with the OEP macrocycle.[95]

Although we were not able to get suitable crystals of (OEP)-Os(CO)(Et_2NNO) for a direct comparison of its structure with the Ru analogue, we were able to obtain suitable crystals of (TTP)Os(CO)(Et_2NNO) for a single-crystal X-ray diffraction

(91) Interestingly, protonation of (OEP)Ru(CO)(Et_2NNO) in CH_2Cl_2 with triflic acid results in the reproducible formation of a small amount (ca. 25%) of [(OEP)Ru(NO)(Et_2NNO)]$^+$ as the only identifiable product. It is likely that the H^+ reagent attacks the coordinated nitrosamine, decomposing it and releasing the NO^+ reagent in situ (ref 23) which then attacks unreacted (OEP)Ru(CO)(Et_2NNO) to give the observed cationic nitrosyl product (as in eq 5). Further examination of this reaction is in progress.

(92) An earlier formulation of osmium nitrosamine complexes formed by oxidation of coordinated ammonia in the presence of secondary amines (ref 93) has been questioned by the same authors (ref 94).

(93) Stershic, M. T.; Keefer, L. K.; Sullivan, B. P.; Meyer, T. J. *J. Am. Chem. Soc.* **1988**, *110*, 6884−6885.

(94) Coia, G. M.; White, P. S.; Meyer, T. J.; Wink, D. A.; Keefer, L. K.; Davis, W. M. *J. Am. Chem. Soc.* **1994**, *116*, 3649−3650, ref 5.

(95) Buchler, J. W.; Kokisch, W.; Smith, P. D. *Struct. Bonding* **1978**, *34*, 79−134.

Table 6. Selected Bond Lengths and Angles for (TTP)Os(CO)(Et_2NNO)

Bond Lengths (Å)			
Os(1)−C(49)	1.818(11)	O(2)−N(5)	1.241(13)
C(49)−O(1)	1.140(12)	N(5)−N(6)	1.294(14)
Os(1)−N(1)	2.052(7)	N(6)−C(52)	1.43(2)
Os(1)−N(2)	2.044(7)	N(6)−C(50)	1.47(2)
Os(1)−N(3)	2.057(7)	C(50)−C(51)	1.41(2)
Os(1)−N(4)	2.068(7)	C(52)−C(53)	1.47(3)
Os(1)−O(2)	2.200(7)		

Bond Angles (deg)			
Os(1)−C(49)−O(1)	177.9(10)	N(5)−N(6)−C(50)	114.2(14)
C(49)−Os(1)−O(2)	174.6(4)	C(50)−N(6)−C(52)	123.9(14)
Os(1)−O(2)−N(5)	115.0(7)	N(6)−C(50)−C(51)	114(2)
O(2)−N(5)−N(6)	113.3(12)	N(6)−C(52)−C(53)	120(2)
N(5)−N(6)−C(52)	121.5(13)		

study. The molecular structure of (TTP)Os(CO)(Et_2NNO) is shown in Figure 6. Selected bond lengths and angles are collected in Table 6. The Os−C(O) and C−O bond lengths are 1.818(11) and 1.140(12) Å, respectively, and the Os−C−O bond angle is 177.9(10)°. To the best of our knowledge, the structure of (TTP)Os(CO)(Et_2NNO) is only the second (por)-Os(CO)-containing structure to be reported to date, the other being (OEPMe_2)Os(CO)(py) (Os−C = 1.828(5) Å, C−O = 1.151(7) Å, Os−C−O = 178.9(14)°).[96] The related phthalocyanine (Pc)Os(CO)(py) complex also has similar Os−CO dimensions (Os−C = 1.83(1) Å, C−O = 1.17(1) Å, Os−C−O = 177(1)°).[97]

The average Os−N(por) bond length in (TTP)Os(CO)(Et_2-NNO) is 2.055 Å and lies within the 2.027−2.069 Å range observed for non-nitrosyl Os^{II} porphyrins.[96,98−100] The nitrosamine ligand is bound to the Os^{II} center in a η^1-O fashion. The axial Os−O(nitrosamine) distance is 2.200(7) Å and is identical to the related Ru−O (axial) distance in (OEP)Ru(CO)(Et_2NNO) (2.199(6) Å). The nitrosamine O−N and N−N bond lengths are 1.241(13) and 1.294(14) Å, respectively, and the nitrosamine O−N−N bond angle is 113.3(12)°. These data are similar to those found in (OEP)Ru(CO)(Et_2NNO). The nitrosamine functionality in (TTP)Os(CO)(Et_2NNO) is essentially planar, with O(2)−N(5)−N(6)−C(52) and O(2)−N(5)−N(6)−C(50) torsion angles of 6.4° and 179.6°, respectively. The nitrosamine ligand nearly eclipses a porphyrin nitrogen (Figure 6b), with a N(4)−Os(1)−O(2)−N(5) torsion angle of −20.2°.

The cationic [(OEP)Os(NO)(Et_2NNO)]BF_4 complex is formed by the reaction of (OEP)Os(CO)(Et_2NNO) with $NOBF_4$ (cf. eq 5). The ν_{NO} of 1800 cm^{-1} is 47 cm^{-1} lower than that of the Ru analogue and is consistent with the greater π-back-bonding capability of Os-to-NO compared with Ru-to-NO.

Epilogue

In summary, we have prepared isolable metalloporphyrin complexes of the group 8 metals containing the diethylnitrosamine ligand. Notably, these complexes are the first isolable nitrosamine complexes of any metalloporphyrin and represent the first crystallographic determination of discrete transition metal nitrosamine complexes displaying the η^1-O binding mode. Further investigations to study (i) the denitrosations of the complexed nitrosamines via release of NO (or NO^+) from these metalloporphyrin complexes and (ii) the oxidative chemistry of the bound nitrosamines[101] are underway. In particular, we are interested in examining the effect of the metal-induced dipolar $^-O-N{=}N^+R_2$ contribution on the decomposition pathways of coordinated nitrosamines.

Acknowledgment. We are grateful to the National Institutes of Health (FIRST Award 1R29 GM53586-01A1) and the National Science Foundation (CAREER Award CHE-9625065) for funding for this research. The support of the Oklahoma Center for the Advancement of Science and Technology is also acknowledged. We also thank Hee-Sun Chung for technical assistance.

Supporting Information Available: Drawings and listings of crystal data, atomic coordinates, anisotropic displacement parameters, bond lengths and angles, hydrogen coordinates and isotropic displacement parameters, torsion angles, and least squares planes (111 pages). Ordering information is given on any current masthead page.

IC9801591

(96) Buchler, J. W.; Lay, K. L.; Smith, P. D.; Scheidt, W. R.; Rupprecht, G. A.; Kenny, J. E. *J. Organomet. Chem.* **1976**, *110*, 109−120.
(97) Omiya, S.; Tsutsui, M.; Meyer, E. F., Jr.; Bernal, I.; Cullen, D. L. *Inorg. Chem.* **1980**, *19*, 134−142.
(98) Che, C.-M.; Lai, T.-F.; Chung, W.-C.; Schaefer, W. P.; Gray, H. B. *Inorg. Chem.* **1987**, *26*, 3907−3911.
(99) Djukic, J.-P.; Young, V. G., Jr.; Woo, L. K. *Organometallics* **1994**, *13*, 3995−4003.
(100) Scheidt, W. R.; Nasri, H. *Inorg. Chem.* **1995**, *34*, 2190−2193.
(101) For example, we have found that the reaction of $[(OEP)Ru]_2$ with diethylnitrosamine in CH_2Cl_2 without the total exclusion of air results in the formation of small amounts of acetaldehyde and diethylamine. Metalloporphyrin-catalyzed aldehyde formation from nitrosamines in the presence of oxidants is not uncommon (ref 102).
(102) Okochi, E.; Mochizuki, M. *Chem. Pharm. Bull.* **1995**, *43*, 2173−2176.